LIGHT SENSITIVITY OF THE ARCTIC COPEPOD *METRIDIA LONGA* DURING MIDNIGHT SUN AND POLAR NIGHT

by

Meaghan Lightfoot

A thesis submitted to the Faculty of the University of Delaware in partial fulfillment of the requirements for the degree of Master of Science in Marine Studies

Spring 2023

LIGHT SENSITIVITY OF THE ARCTIC COPEPOD *METRIDIA LONGA* DURING MIDNIGHT SUN AND POLAR NIGHT

by

Meaghan Lightfoot

Approved: _____
Jonathan H. Cohen, Ph.D.
Professor in charge of thesis on behalf of the Advisory Committee

Approved: _____
Katharina Billups, Ph.D.
Chair of the School of Marine Science and Policy

Approved: _____
Fabrice Veron, Ph.D.
Dean of the College of Earth, Ocean, and Environment

Approved: _____
Louis F. Rossi, Ph.D.
Vice Provost for Graduate and Professional Education and
Dean of the Graduate College

ACKNOWLEDGMENTS

I would firstly like to thank Dr. Jonathan Cohen for his continued support of my research. Without his insight, this project would not have been possible. I appreciate his time and efforts in this project, as well as his patience and willingness to help. A further thank you to my committee members, Dr. Kim Last and Dr. Mark Moline, for their feedback and advisement of this project. Specifically, Dr. Last was a huge help during sampling in Ny-Ålesund. Thank you to the crew of the R/V Helmer Hanssen for their flexibility and rigor during sampling, especially when times got tough this past January. I also want to acknowledge the scientific support I received on the boat, specifically from Malin Daase, whose expertise on Arctic copepods helped exponentially in working with *Metridia longa* during both cruises.

I received so much support from my lab mates and friends Hayden Boettcher, Taylor Hoffman, and Julia Fontana. Meeting and working with them over the past 2 years has been one of my best experiences, and I am so thankful to have them in my life. An additional thanks to my family, specifically my mom, dad, sister Riley, and grandparents, as well as my friends back in Maryland and Ohio. Without every single one of you, none of this would have been possible. Thanks for always being there for me, and especially for answering the phone in my times of need.

TABLE OF CONTENTS

LIST OF TABLES

LIST OF FIGURES

ABSTRACT

The Arctic is defined by a seasonal light regime extending between 24-hour light (Midnight Sun) and 24-hour dark (Polar Night). Light itself acts as an important cue for marine zooplankton, dictating their orientation/navigation and vertical migration, prey detection and predator avoidance, and population dynamics/reproductive strategies. Changes in the spectral, intensity, and duration components of downwelling irradiance during Midnight Sun and Polar Night contribute to the annual Arctic light climate, and to what characteristics of light are used for zooplankton visual processes. Additionally, as the Arctic region is warming at an alarming rate, the loss of annual sea ice and snow coverage is projected to increase incoming illumination into the water column, impacting zooplankton visual systems, trophic dynamics, and predator-prey interactions.

Given the marked differences in annual light climate at high latitudes, the objective of this study was to determine the behavioral responses of zooplankton species to spectral and irradiance light stimuli during Midnight Sun and Polar Night. The copepod species *Metridia longa* copepods were selected as the target species for this research due to their biomass in Atlantic-Arctic waters, vertical migration behaviors, and bioluminescent capabilities. While Polar Night twilight peak emissions are blue dominant (λ_{max} = 455 nm) there is a shift towards green light (λ_{max} = 550 nm) availability during Midnight Sun due to spring phytoplankton blooms and suspended particulate matter in the water column. Therefore, it was hypothesized that copepods

will exhibit a broad spectral response sensitivity in the blue-green wavelengths in order to compensate for the annual shifts in available spectra. Additionally, it is expected that *M. longa* copepods will have a heightened irradiance response during Polar Night compared to Midnight Sun. Zooplankton visual systems are often more sensitive in low light conditions, thus it is hypothesized that irradiance responses will be increased during Polar Night.

Sampling took place in the Barents Sea in May 2022 (Midnight Sun) and January 2023 (Polar Night), with additional sampling in Kongsfjorden during Polar Night in January 2023. Light response/sensitivity was assessed on an individual basis in this study to provide insight into the individual variability in light sensitivity among *M. longa* copepods. This was accomplished using an adjustable, high throughput apparatus to test 64 individual zooplankton swimming behavior individually and simultaneously to spectral and irradiance light stimuli.

Results suggest a consistent blue-green dominant spectral response between Midnight Sun and Polar Night to wavelengths ranging from 400 to 550nm, along with an increased irradiance response by an order of magnitude among Polar Night copepods compared to those tested during Midnight Sun. Additionally, irradiance response among *M. longa* copepods may vary with developmental stage, but are not dependent on location or temperature during Polar Night. From these results, it was determined that *M. longa* female copepods can detect light down to 119 m during Midnight Sun in the Barents Sea and 55 m in Kongsfjorden during Polar Night. These irradiance thresholds correspond to reported depths of zooplankton across seasons as they move vertically with isolumes.

In a changing Arctic, loss of sea ice and snow attenuating incoming irradiance is predicted to increase the pelagic visual lightscape. Since light sensitivity was not temperature dependent in this study, thresholds of detectable light in the water column should not vary with climate change-related increases in water temperature. This suggests that zooplankton like *M. longa* may be forced deeper in the water column to maintain themselves in darkness. Future work should assess *M. longa* response sensitivities under a more climate-focused lens, and incorporate additional components like cameras and other sensor positions to the apparatus created for this study to provide a full picture to zooplankton behavior in response to light at high latitudes

Chapter 1

GENERAL INTRODUCTION

Light acts as a cue for major marine biological processes. Its availability in the water column impacts photosynthetic activity and primary production, circadian rhythms, use of bioluminescence, and diel vertical migration (DVM), subsequently influencing biogeochemical transport processes (Castellani et al., 2022; Häfker et al., 2022). Vision and light response in marine animals aids in predator avoidance and prey detection, mating and reproduction, and navigation and spatial detection (Warrant & Johnsen, 2013).

Light driven biological processes are dictated by the spectral and intensity components of irradiance. In biological studies, spectral irradiance is commonly integrated between 400 nm and 700 nm and denoted as E_{PAR}, providing an irradiance value with relevance to both photosynthetic activity and vision. Additionally, through the optical properties of absorbance and scattering, irradiance loses intensity with depth, creating an isolume in the water column, or a depth varying level of constant light intensity (Kirk, 2010). Light sensitivity of marine organisms, the light organisms see and therefore respond to, is dictated by these spectral and irradiance intensity components of light in marine environments. Light spectra and intensity, together with photoperiod, contribute to what is known as the light climate in the Arctic.

The poles represent global extremes in light climate. In the Arctic, light climate is defined by seasonal periods of 24-hour light (Midnight Sun) and 24-hour dark (Polar Night), resulting in annual changes to the overall intensity and spectral

characteristics of available irradiance (Fig. 1.1) (Cohen et al., 2020; Connan-McGinty et al., 2022). The light periods are characterized by the sun's continued position above (Midnight Sun) or below (Polar Night) the horizon. Additionally, Polar Night is experienced differently depending on latitudinal position and time of day; increases in latitude are proportional to increases in the sun's elevation below the horizon. Thus, Polar Night is defined from lower (64.7°N, start of the Arctic Circle) to higher latitudes in the Arctic as polar twilight (64.7°N to ~72°N), civil Polar Night (72°N to ~78°N), nautical Polar Night (78°N to ~84°N) and astronomical Polar Night (> 84°N). This means Polar Night is not continually dark, but rather consists of twilight dependent on latitudinal position, lunar irradiance, and light from the aurora borealis (Cohen et. al, 2020). Additionally, these descriptions correspond to the darkest light period experienced in each respective zone. Continued diel changes in solar elevation are another component to the light climate experienced during Polar Night (Berge et al., 2020a). The same is true for Midnight Sun, daily changes in the sun's positioning above the horizon result in lower light availability/intensities at midnight compared to midday (Leu et al., 2016; Pavlov et al., 2019). The Arctic, therefore, is an ideal location for understanding how marine zooplankton behavior changes in response to light availability, both the spectral and intensity characteristics of available light, in a given year.

The underwater light climate in the Arctic is also heavily influenced by phytoplankton blooms, sea ice, and snow coverage. These factors are the major light attenuating forces in the region. Sea ice attenuates light ten times more effectively compared to the open ocean, and snow even more so in comparison to sea ice (Castellani et al., 2022). With the Arctic undergoing rapid warming due to the effects

of global climate change, studies estimate a time shift in seasonal algal blooms (Castellani et al., 2022), and areas such as the Barents Sea, are projected to be ice free by 2036 (Onarheim & Årthun, 2017). Varpe et al. (2015) predicts drastic increases in underwater light intensities with modeled Arctic sea ice loss by 2040. Increased illumination in the water column may impact zooplankton communities through increased visual predation risks (Langbehn & Varpe, 2017; Varpe et al., 2015) and changes to zooplankton visual systems (Viljanen et al., 2017), impacting their light mediated behaviors.

In zooplankton, visual systems aid in the photon capture of biologically relevant light for biological processes. For copepods specifically, their naupliar eye is simple and located in the central anterior position on the head. It can consist of three cups, two lateral and one ventral, each containing a lens, tapetum, and rhabdom photoreceptor cells, but has diversified among copepod species. Some species contain three separate eye structures, and variations in lens size (if present) and photoreceptor cells exist across copepod taxa (Porter et al., 2017). Tapetal cells in some naupliar eyes aid in light reflection and increase light sensitivity (Martin et al., 2000), and the naupliar eye as a whole is also theorized to be useful in light detection and provides some degree of spatial orientation (Porter et al., 2017).

Metridia longa copepods were chosen as a target model species in this study. They are one of the more prominent Arctic copepod species in terms of biomass, vertical migration, and importance (Berge et al., 2020b, 2014; Daase et al., 2008) (Fig. 1.2). They are also a major bioluminescent species, contributing heavily to Arctic bioluminescent light availability at increased depths. Cronin et al. (2016) found that *M. longa* contributed the majority of bioluminescent light past 40 m during Polar

Night in Kongsfjorden. They have been noted to be active throughout the summer, with older copepodite stages and adult females still showing elevated activity and migration during the winter (Båmstedt & Tande, 1988; Daase et al., 2008). I therefore present *M. longa* copepods as an ideal model for understanding light response behavior among Arctic copepods.

The main objective of this study is to determine the light sensitivity, i.e. spectral and irradiance response sensitivities, of the Arctic copepod *Metridia longa* during Midnight Sun and Polar Night. I hypothesize that *M. longa* will exhibit a blue-green dominant spectral response sensitivity in both periods. In contrast, I expect these copepods to show heightened irradiance response during Polar Night compared to Midnight Sun. Additionally, further Polar Night sampling allowed for light sensitivity and activity to be analyzed in the context of stage (copepodite stage V and adult females), location (shelf vs. fjord), time (day vs. night) and temperature (6 °C vs. -1°C).

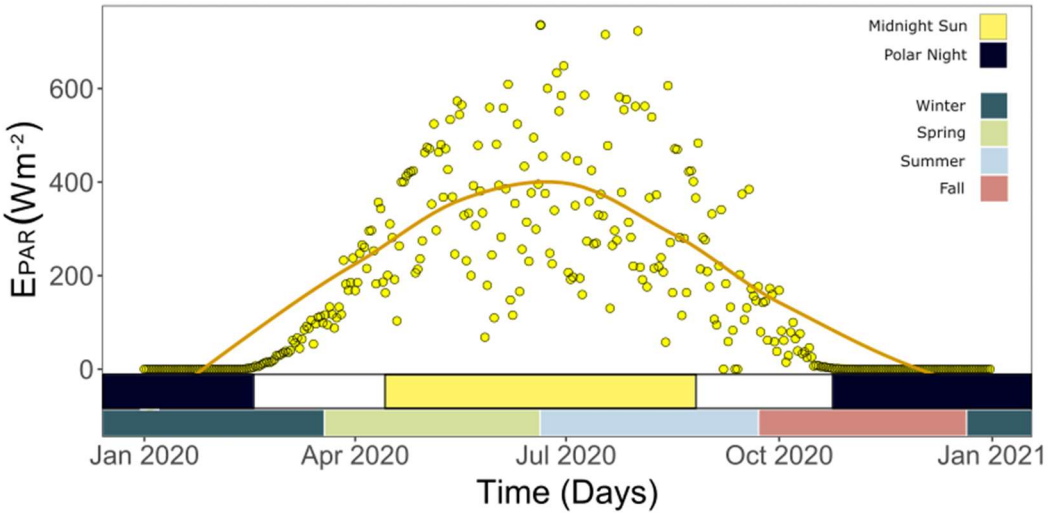

Figure 1.1: Annual variations in available irradiance between Midnight Sun and Polar Night. Irradiance in the photosynthetically active radiation range (integration of light from 400 to 700nm) is plotted as a function of time for the year 2020 in Ny-Ålesund, Svalbard. Polar Night (dark blue blocks) and Midnight Sun (yellow block) are the periods where the sun's elevation relative to the horizon, below or above respectively, remains consistent throughout the diel shift from day to night. Additionally, the changes in season, winter (dark green), spring (light green), summer (light blue), and fall (pink), are plotted over the year in relation to when Midnight Sun and Polar Night occur, further impacting the spectral characteristics of available light in the given year/each light period.

Figure 1.2: Female *Metridia longa* copepod.

Chapter 2

ASSESSING THE SPECTRAL AND IRRADIANCE REPONSES OF *METRIDIA LONGA* COPEPODS DURING MIDNIGHT SUN AND POLAR NIGHT

2.1 Introduction

The Arctic region experiences seasonal variations in light availability due to annual shifts in solar elevation (Cohen et al, 2020). Spectral irradiance subsequently differs during the light periods of Midnight Sun, 24-hour light, and Polar Night, 24 hour-dark (Connan-McGinty et al., 2022). Due to the implementation of the ArcLight light observatory outside of Ny-Ålesund, Svalbard (79°N), high resolution light measurements have been used to reveal the differences in light intensity across E_{PAR} during Midnight Sun and Polar Night. Johnsen et al. (2021) reports averaged daily maximum intensities of 1136 to 1398 μmol photons cm^{-2} s^{-1} (6.84 - 8.42 x 10^{16} photons cm^{-2} s^{-1}) and minimum intensities of 4.1 - 5.3 x 10^{-6} μmol photons cm^{-2} s^{-1} (2.47 - 3.19 x 10^{8} photons cm^{-2} s^{-1}) across a 4-year timeframe, both corresponding respectively to Midnight Sun and Polar Night. Additionally, Grant et al. (2023) used ArcLight to denote changes across the visible spectrum throughout the year and with solar elevation/angle. They report that summer (Midnight Sun) clear day measurements coincide with a peak spectral output of 460 nm. Additionally, the relative proportion of red light increases when the sun is below the horizon at twilight and during Polar Night (Grant et al., 2023).

Midnight Sun spectral attenuation in the water column are also impacted by the presence of colored dissolved organic matter (CDOM), suspended particulate matter, and spring phytoplankton blooms (Castellani et al., 2022, Hancke et al., 2014; Volent

et al., 2007). CDOM, particulate matter, and phytoplankton all absorb blue light, absorbance decreasing exponentially into the greens and reds for CDOM, but increasing in the reds for phytoplankton (Grant et al. 2023; Castellani et al., 2022; Siegel et al., 2002), leaving a scattering effect of green light in the environment. Similar to sky light spectral output during Midnight Sun as reported by Grant et al. 2023, a spectral peak at 455 nm was measured at solar noon during Polar Night by Cohen et al. (2015a). The study also models spectral light availability with depth, finding a 465 nm peak at 10 m and a shifted 485 nm peak beyond 30 m (Cohen et al., 2015a).

Behavioral responses to light among zooplankton species have been previously quantified using experimental systems consisting of continuous video recordings of grouped animal behavior to various light stimuli in clear troughs (Båtnes et al., 2015; Buskey & Swift, 1985; Cohen & Forward, 2002) or by monitoring movement in partition troughs (Buskey et al., 1989). However, individual variability in responses to light stimuli has not been extensively researched. It is well documented that not all individuals participate in daily DVM behaviors (Mehner & Kasprzak, 2011; Ogonowski et al., 2013), and is further asynchronous during Midnight Sun/limited in Polar Night (Hobbs et al., 2021). Methods used in Kennedy et al. (2022) allowed for individual data collection with wavelength and intensity control, but could only test six individuals at once with non-optimal temperature control methods (ice packs used to maintain low temperatures). In this study, the swimming activity in relation to spectral and irradiance light stimuli was assessed using a compact apparatus, easy for set up in light and temperature-controlled environments, and able to collect data

individually and simultaneously for 64 copepods (scalable to many more) in a short time span.

My focal species for this study is the Arctic copepod *Metridia longa*. Previous research on the light sensitivity of *M. longa* includes Buskey & Swift (1985) in which photobehavioral responses in relation to 60 ms flashes of different wavelengths, ranging from 420 to 620 nm, was assessed for groups of 5 copepods off the coast of Iceland in summer, finding an increased response from 460 to 520 nm. The study also noted that *M. longa* copepods showed a strong swimming response to simulated bioluminescent flashes at 475 nm, 2.0 $\mu E\ m^{-2}\ s^{-1}$ light intensity. Additionally, Daase et al. (2008) found that their vertical distribution in the water column is often dictated by light intensity preference and developmental stage, older copepods found higher in the water column at night compared to daytime, while juveniles remain at depth regardless of light conditions.

To build off these results, I studied the spectral and irradiance response behavior of *M. longa* females across light periods at high Arctic latitudes. Additionally, I assess light sensitivity in relation to location during Polar Night, assessing response between Barents Sea shelf water individuals (75°N, civil Polar Night) and individuals sampled at a western Svalbard fjord location (79°N, nautical Polar Night). Light sensitivity was also quantified across copepodite stage (CV vs. adult females), time of day (day vs. night), and temperature; all parameters missing from the current literature available on *M. longa* light response.

2.2 Methods

2.2.1 Collection of *Metridia longa* Copepods

Sampling took place from May 18 - 27, 2022 (Midnight Sun) and January 6 - 16, 2023 (Polar Night) in the Barents Sea at 74.59°N 29.05°E (Midnight Sun - Shelf, hereafter MS-S) and 75.00°N 15.11°E (Polar Night - Shelf, hereafter PN-S) respectively from the R/V Helmer Hanssen. Further Polar Night sampling was conducted in Kongsfjorden, Svalbard at 78.96°N 11.96°E (Polar Night - Fjord, hereafter PN-F) from January 17 - 27, 2023 on the M/S Teisten (Fig. 2.1). The copepod *M. longa* were collected using a 1 m^2, 1000 µm mesh Tucker trawl towed at 250 m on May 23, 2022 (MS-S), a 253 µm mesh WP2 net hauled vertically from 300 m to the surface on January 12, 2023 (PN-S), and a 1000 µm mesh WP3 net hauled vertically from 150 m to the surface on January 17 and 24, 2023 (PN-F). CTD casts (Sea-Bird SBE 9 on R/V Helmer Hanssen, SBE 37-microCAT on M/S Teisten) were conducted at each station for collection of temperature and salinity across the sampled water column. Cosine-corrected downwelling irradiance measurements across the photosynthetically active radiation range (hereafter referred to as $E_{d,PAR}$, integrated across 400 to 700 nm) were also taken on May 23, 2022 at 9:30 am local time at MS-S (Satlantic PAR Sensor) and January 18, 2023 at 11:00 am local time at PN-F (Biospherical Instruments MPE PAR Sensor) for an understanding of differences in overall light availability between periods. Once copepods were collected, cod ends were rinsed into darkened buckets and samples immediately transferred to dark cold rooms (3 - 4°C in the Barents Sea, 2°C in Kongsfjorden). Individual *M. longa* were identified under dim red light using a microscope and placed separately in 5 mL tubes, each containing 3 mL of station-specific filtered seawater (0.7 µm MS-S; 2.0 µm

PN-S, 0.2 μm PN-F) that matched each stations' ambient temperature and salinity (except in temperature experiments, see below). Once in tubes, individuals were transferred to experimental chambers, described in detail below, and left to dark acclimate for one hour before experimental trials began.

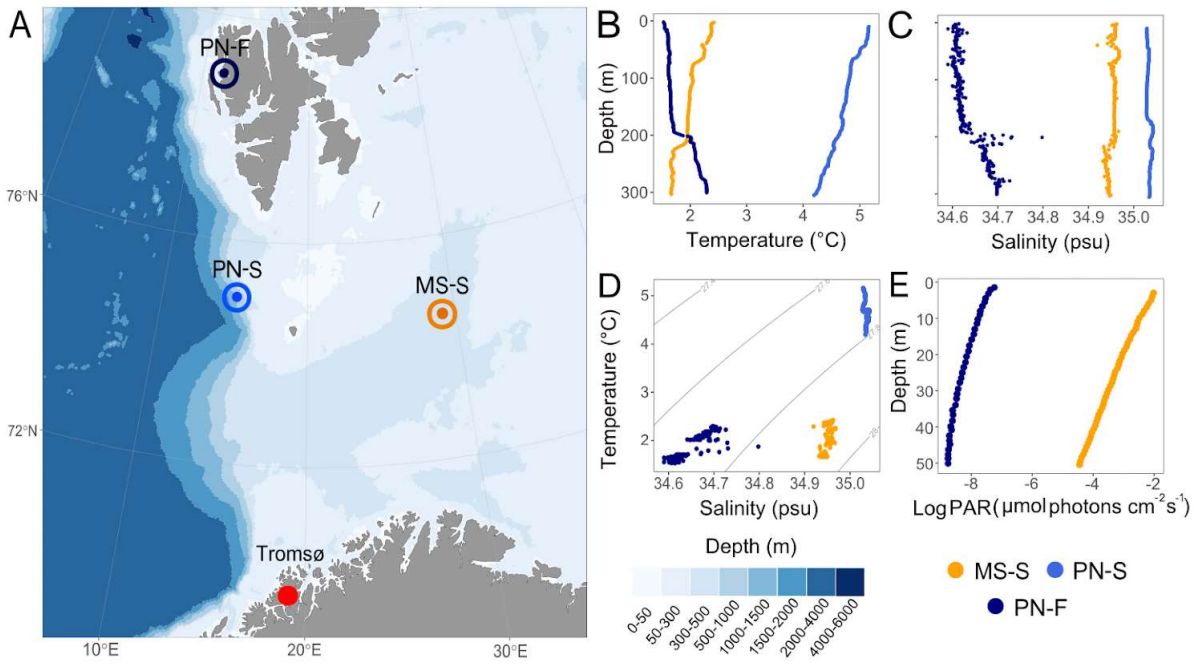

Figure 2.1: Sampling Stations of *Metridia longa* Copepods During Midnight Sun and Polar Night. The map details **(A)** sampling stations during Midnight Sun and Polar Night, both in the Barents Sea Atlantic Shelf and Kongsfjorden. Station names, which include both the sampling season and location, are Midnight Sun Shelf (MS-S, orange), Polar Night Shelf (PN-S, blue), and Polar Night Fjord (PN-F, dark blue). Also included are **(B)** temperature and **(C)** salinity profiles for Stations MS-S, PN-S, and PN-F, as well as a **(D)** temperature vs. salinity plot for each station. **(E)** Cosine-corrected E_{PAR} measurements (Satlantic PAR Sensor [MS-S], Biospherical Instruments MPE PAR Sensor [PN-F]) were also taken during Midnight Sun and Polar Night.

2.2.2 Experimental Apparatus

I optimized a high-throughput apparatus for light (spectral and intensity) stimulation and simultaneous measurement of swimming activity in individual *M. longa* copepods (Fig. 2.2). The apparatus consists of a high intensity light source (ThorLabs OSL2 with 150W EJV halogen bulb, ThorLabs OSL2B2) connected to two motorized filter wheels (ThorLabs FW102C), each containing six, one-inch filter positions, to expose copepods to various wavelengths and intensities of light. Light is directed from the lamp to the wheels through an attached fiber cable (6.4 mm core diameter) that fits to a collimation tube (ThorLabs OSL2COL) containing a 12mm plano convex lens (focal length = 30mm). This focuses the light through the first wheel opening, which is collimated again using a 25mm plano convex lens (focal length = 50mm, ThorLabs LA1131) held within a lens tube attaching the two filter wheels together. The second convex lens is critical to focus incoming light through the second filter wheel opening onto the attached liquid light guide (approximately 1.5 meters, 8mm core diameter, held using ThorLabs AD8F adaptor and CP33 cage plate) that delivers the light stimulus to the activity monitors (described below). An electromagnetic shutter (ThorLabs SHB15T) controls the timing of light exposure. The collimation tube is attached to the shutter through a 25mm externally threaded coupler (ThorLabs SM05T10).The shutter itself is positioned on the first filter wheel external housing using a cage plate mount (ThorLabs, SHCP05) placed over the opening to the first filter. An AD Instruments 26T Series PowerLab controls the shutter driver along with both filter wheels, programmed to both open and close the shutter and position the correct filters through preset TTL pulses within a custom control routine created in the LabChart software.

Animal activity was recorded by two locomotor activity monitors (LAM25, TriKinetics Inc., hereafter LAMs) placed in light-tight temperature-controlled enclosures where experiments took place (either reach-in incubator or walk-in environmental room). LAMs were positioned under a central liquid light guide that was maneuvered through holes at the side of the enclosure and positioned within incubator shelves/prepared rods to ensure the light source stays in place. A KimWipe tissue was positioned on the end of the liquid light guide to diffuse the emitted light. Each LAM contained 32 evenly spaced 25mm diameter holes, with each hole fitting a 75 mm x 10 mm test tube for a total 64 animals exposed to the wavelengths and intensities exposures. Copepod movement within each tube was tracked using 3 pairs of infrared beams positioned uniformly around the bottom portion of each test tube and recorded as counts at the time an animal crosses its individual beam array in the DAM System software with a resolution of 2 s.

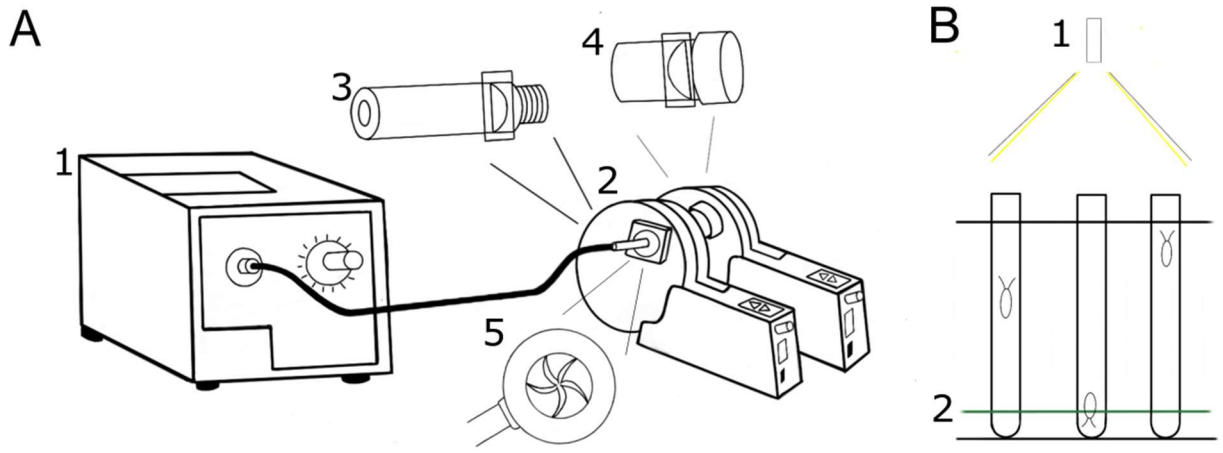

Figure 2.2: Schematic of the Light Stimulus and Locomotor Activity Monitors. Schematic of the **(A.1)** high intensity lamp (ThorLabs OSL2B2 with 150W EJV halogen bulb, ThorLabs OSL2B2) connected to **(A.2)** two motorized filter wheels (ThorLabs FW102C) through a 6.4mm fiber adaptor. The adaptor fits into a **(A.3)** collimation tube (ThorLabs OSL2COL) containing a 12mm plano convex lens (focal length = 30mm) to focus light through the first filter wheel. The wheels are attached using a **(A.4)** 25mm lens tube, also containing a 25mm plano convex lens (focal length = 50mm, ThorLabs LA1131) to focus incoming light through the second wheel and onto a liquid light guide attached to the other side. **(A.5)** An electromagnetic shutter (ThorLabs SHB15T), connected to the outside of the first filter wheel, controls the timing of light exposure. From the outside of the second wheel, a liquid light guide is attached. The light guide can be maneuvered into experimental chambers and is **(B.1)** located vertically above two locomotor activity monitors (LAMs). Each LAM contains 32 evenly spaced test tube positions, with a **(B.2)** sensor plate containing infrared beams positioned approximately 15 mm from the bottom of each test tube to record movement.

2.2.3 Experimental Design

Two types of experiments were conducted during the Midnight Sun and Polar Night periods, (1) spectral response and (2) irradiance response. Spectral response was measured by exposing copepods, in the LAM systems, to wavelengths ranging from 400 nm to 670 nm, increasing each by 30 nm, at an average intensity of 1.96 x 10^{10} photons $cm^{-2}s^{-1}$ during Midnight Sun and 1.19 - 1.27 x 10^{10} photons $cm^{-2}s^{-1}$ during Polar Night. This value was chosen through consideration of the sensitivity thresholds of other migratory zooplankton species; irradiance response thresholds of other polar zooplankton typically falling in the range of 10^{6} to 10^{12} photons $cm^{-2}s^{-1}$ to blue-green light stimuli (referred to in the discussion, Table 2.5). This is a wide range of thresholds, and the ideal irradiance value would be high enough to initiate a response above the organism's threshold value to blue-green light, not only to ensure general response, but also to ensure response across all tested wavelengths. Therefore, a value of 10^{10} photons $cm^{-2}s^{-1}$ was selected, and extensively tested in preliminary spectral experiments on light responsive organisms in the DE Bay (*Acartia tonsa* and *Centropages* spp. copepods and *Neomysis americana* mysids). Additionally, in irradiance response experiments, this intensity corresponds to the second highest intensity exposure (see below). Further preliminary DE Bay testing also validated the order in which copepods were exposed to light stimuli, in which no difference in response was quantified in *N. americana* individuals when exposed to wavelengths in reverse order from red light to blue (670 to 400 nm).

Quantal irradiance in spectral response experiments was matched to that at 400 nm using fixed neutral density filters (see section 2.2.3.1 Light Calibration). In an experiment, copepods received two, one minute light increments per wavelength, with a minute of dark between similar exposures and five minutes of dark between different

exposures. Spectral response of *M. longa* copepods was tested during Midnight Sun and Polar Night at all sampling stations (MS-S, PN-S, and PN-F) for a total of three experiments (Table 2.1). Apart from a comparison between the spectral response of *M. longa* copepodite stage 5 and adult female stages during the Polar Night (PN-S), males and younger copepodite stages were removed from experimental analysis as too few were tested to evaluate their behavior.

Irradiance response was measured in a similar method to spectral. In this experiment, copepods were exposed to increasing intensities of light at 490 nm, irradiance increasing half an order of magnitude with each exposure. Intensities ranged from 2.70×10^5 to 9.27×10^{10} photons $cm^{-2}s^{-1}$. The timing of an irradiance experiment was the same as that described above for spectral experiments. A total of seven irradiance experiments took place during Midnight Sun and Polar Night (Table 2.1).

2.2.3.1 Light Calibration

In spectral experiments, copepods were exposed to similar intensities of light across wavelengths (400 - 670 nm) (i.e., *response spectrum* experimental design). Wavelength filters were quantaly matched through spectral irradiance measurements (Ocean Optics QE Pro spectroradiometer with a cosine-corrected optical fiber) taken at each test wavelength. Neutral density filters, optical densities ranging from 0.7 to 1.15, were then assigned to the 430 to 670 nm spectral filters in order to match the approximate throughput intensity at 400 nm.

In irradiance experiments, animals were exposed to increasing intensities of light at 490 nm, with intensity controlled by neutral density filters. Irradiance at 490 nm without neutral density filters was measured at the center of the LAM field using a

radiometrically-calibrated energy sensor with flat spectral response (Gamma Scientific, UDT model 247). Irradiances at 490 nm for different combinations of neutral density filters were then calculated based on this value and transmission percentage of each optical density (OD) by taking ten to the power of the negative value of the OD. These values were then multiplied by the initial 0 OD intensity value to calculate the transmitted central irradiance value per applied neutral density filter. Energy values ($\mu W\ cm^{-2}$) were then converted to photons $cm^{-2}s^{-1}$ by dividing watt values by 1×10^{6} and multiplying this new value by 490 divided by 1.987×10^{-16}.

Light measurements were also taken at each LAM test tube position to ensure an even distribution of light across the LAM field. I made these measurements at each sampling station (MS-S, PN-S, PN-F) since each involved disassembly and reassembly of the experimental apparatus. Additionally, this ensured light exposures were similar across stations and sampling periods. Position measurements were taken as described above for irradiance experiments, both under white light (UDT energy measured at 500 nm) and at 490 nm. For all relevant experiments, a linear regression model was run between each individual's summed beam breaks at the overall group's peak response point (a wavelength or intensity) and each individual's assigned intensity per their LAM position. Regression results indicate no relationship between individuals' responses and their assigned LAM positions/intensity value, confirming that LAM positions did not systematically bias responses (Fig. A1).

2.2.3.2 Analysis

After experiments were completed, pictures of each individual tested were taken. From pictures, individuals were confirmed as *M. longa* copepods and copepodite stage and sex of adults was determined by the number of urosome

segments (Klekowski et al., 1991). Measurements of prosome and total copepod length were conducted in ImageJ software to gain insight into the mean size of individuals tested.

Spectral experiments were analyzed using a non-parametric repeated measures ANOVA (Friedman Test), comparing each individual's beam break sums per light interval to their average dark activity. Beam break sums and dark activity values were normalized per individual to understand overall trends in spectral response. The activity values for each wavelength stimuli include the two-minute light exposures, plus the one-minute dark periods following each stimulus (4 minutes total per stimulus). Dark control values consist of a grand mean of every individual's averaged activity across the prior 4-minute dark periods in an experiment. Statistical differences between response at each wavelength and the average dark activity were quantified using a post hoc paired Wilcoxon signed rank test with a Holm-Bonferroni p-value correction (Zar, 2010).

Irradiance experiments were analyzed in the same manner as spectral results. However, activity in irradiance experiments was not normalized per individual. I observed clear differences in dark control and photoresponse activity between irradiance experimental comparisons. Subsequently, differences in activity between dark controls were analyzed using a Wilcoxon rank sum test or one-way ANOVA (Kruskal-Wallis test) with a post-hoc Dunn's test.

Irradiance results were further analyzed at the individual copepod level using a 4-parameter logistic dose-response analysis. The logistic model was first performed on the mean response of all tested individuals per light intensity, and the estimated half-saturation parameter was used to identify the group's irradiance threshold. A

model was then fit for every individual's response across the exposed light intensities. This was used to identify individuals whose curves showed significant model fits, and in turn irradiance thresholds. A mean log transformed threshold value per experiment was then calculated using only significant individuals, and back transformed into a photon value. Additionally, significant irradiance thresholds on the individual level were then compared across experimental trials using either a Kruskal-Wallis ANOVA with a post hoc Dunn's test or a Wilcoxon rank sum test.

.

Table 2.1: Light Sensitivity Experiments Conducted during Midnight Sun and Polar Night. The table below details the types of experiments performed during Midnight Sun and Polar Night and their respective location. The total number of individuals column includes the number of *M. longa* copepods tested in each experiment. Stage columns, however, only detail the number of copepods viable for analysis (i.e. showed response in an experiment. Individuals who did not show any activity throughout an experiment were removed from analysis). Additionally, due to low sample numbers, results from CIV and adult male copepods are not included in this study. CV copepods are only analyzed in comparison to females at the PN-S station. Mean prosome and total length (± standard deviation) per stage and experiment are also detailed below.

Season	Station	Experiment	Total Individuals (#)	CIV (#)	PL (mm) ± sd; TL (mm) ± sd	CV (#)	PL (mm) ± sd; TL (mm) ± sd	Males (#)	PL (mm) ± sd; TL (mm) ± sd	Females (#)	PL (mm) ± sd; TL (mm) ± sd
Midnight Sun											
	MS-S	Spectral Response	81	(0)		(0)		(1)	**2.46**; **3.75**	76	**2.56** ± 0.14; **4.05** ± 0.25
	MS-S	Irradiance Response	60	(0)		(0)		(1)	**2.54**; **4.22**	55	**2.59** ± 0.09; **4.15** ± 0.18
Polar Night											
	PN-S	Spectral Response	59	(5)	**1.38** ± 0.05; **2.06** ± 0.08	(17)	**1.90** ± 0.19; **2.94** ± 0.59	(15)	**1.87** ± 0.36; **3.15** ± 0.60	20	**2.61** ± 0.1; **4.27** ± 0.17
	PN-S	Irradiance Response	42	(0)		(14)	**1.93** ± 0.02; **3.07** ± 0.06	(4)	**2.00** ± 0.08; **3.38** ± 0.18	21	**2.61** ± 0.15; **4.23** ± 0.28
	PN-F	Spectral Response	40	(0)		(0)		(0)		40	**2.53** ± 0.18; **4.15** ± 0.34
	PN-F	Irradiance Response	44	(0)		(0)		(0)		40	**2.57** ± 0.19; **4.28** ± 0.35
	PN-F	Daytime Irradiance Response	38	(0)		(1)	**1.92; 3.08**	(1)	**2.58; 3.95**	35	**2.54** ± 0.14; **4.18** ± 0.22
	PN-F	Nighttime Irradiance Response	44	(0)		(3)	**2.25** ± 0.23; **3.59** ± 0.37	(0)		38	**2.49** ± 0.20; **4.10** ± 0.34
	PN-F	6 °C Irradiance Response	41	(0)		(1)	**1.90**; **3.34**	(0)		38	**2.40** ± 0.20; **3.95** ± 0.36
	PN-F	-1 °C Irradiance Response	59	(0)		(0)		(0)		56	**1.44** ± 0.27; **3.35** ± 0.59

2.3 Results

2.3.1 Environmental Context

Temperature and salinity profiles were averaged across sampling depth per station. Barents Sea temperatures were on average 2.06°C across the sampled 250 m during Midnight Sun (MS-S) and 4.7°C across 300 m during Polar Night (PN-S). Average fjord (PN-F) temperature across the 150 m sampling depth was 1.62°C (Fig. 2.1B). Accordingly, experimental temperatures for seasonal comparisons were set for 2-3 °C, with temperature loggers in experimental chambers recording on average:1.8°C (MS-S), 3.0°C (PN-S), and 1.7°C (PN-F). Average salinities in the Barents Sea were 35.0 psu for both Midnight Sun and Polar Night, and 34.6 psu at PN-F (Fig 1C).

Light measurements show a distinct difference in light availability between Midnight Sun and Polar Night (Fig. 2.1E). Measurements taken just below the surface show a five order of magnitude difference in $E_{d,PAR}$, 2.76 x 10^{-2} µmol photons cm^{-2} s^{-1} during Midnight Sun and 1.12 x 10^{-7} µmol photons cm^{-2} s^{-1} during Polar Night. At 10 m, PAR values were 2.9 x 10^{-3} and 1.66 x 10^{-8} µmol photons cm^{-2} s^{-1} and, at approximately 50 m, values were down to 3.6 x 10^{-5} and 1.73 x 10^{-9} µmol photons cm^{-2} s^{-1}. Attenuation coefficients per season, calculated over 3m to 40 m depth, were 0.120m^{-1} and 0.079m^{-1} for Midnight Sun and Polar Night, respectively.

2.3.2 Spectral and Irradiance Response During Midnight Sun vs. Polar Night

In spectral response experiments, *M. longa* showed a blue-green dominant response across Midnight Sun and Polar Night periods. Females tested at the MS-S station during Midnight Sun (n = 76) exhibited increased swimming activity relative to dark control from 400 to 550 nm (Fig. 2.3A) (Table 2.2). For Polar Night, PN-S

(n=20) and PN-F (n=40) females were combined as both locations showed 400-520 nm sensitivity (Table 2.2, Fig. 2.3B; for PN-S vs. PN-F see Fig. B1).

In irradiance response experiments conducted at 490 nm (wavelength for all subsequent irradiance experiments), MS-S females (n = 55) have swimming activity exceeding dark controls (i.e., irradiance threshold) beyond 3.40 x 10^9 photons $cm^{-2}s^{-1}$ when analyzing using the repeated measures method (Table 2.3) (Fig. 2.4A). PN-S females (n = 21), however, do not show a significant increase in swimming activity over dark controls at any irradiance level, although a step increase in activity may be present at 9.27 x 10^8 photons $cm^{-2}s^{-1}$ (Fig. 2.4B). PN-F individuals, in comparison, responded significantly beyond 8.76 x 10^9 photons $cm^{-2}s^{-1}$ (Table 2.3) (Fig. 2.4C). More prominent, however, is the change in overall activity observed between periods, MS-S females seemingly responding more than PN-S and PN-F females. The activity analysis between each experiment's individuals' baseline dark movement revealed median response among MS-S individuals was higher (3.417 beam breaks/48 min) than PN-S (3.083 beam breaks/48 min) and PN-F (3.042 beam breaks/48 min) individuals (Fig 2.4D). Further analysis of photoresponse between MS-S and PN-F groups at their respective irradiance thresholds also showed increased copepod activity during Midnight Sun, (MS-S: median response of 7 beam breaks/48 minutes vs. PN-F: median response of 5 beam breaks/48 minutes). Between the Polar Night locations, baseline dark activity is comparable, but photoresponse is seemingly higher in the fjord (PN-F) vs. the shelf (PN-S).

Irradiance thresholds were also identified by fitting 4-parameter logistic dose-response models to the mean swimming response in a given experiment (Fig. 2.5). Thresholds correspond to the curve's estimated intensity value at half-saturation.

During Midnight Sun and Polar Night, estimated thresholds are 2.70 x 10^9 photons $cm^{-2}s^{-1}$ for MS-S (Fig. 2.5A), 6.37 x 10^8 photons $cm^{-2}s^{-1}$ for PN-S (Fig 2.5B), and 2.22 x 10^9 photons $cm^{-2}s^{-1}$ in PN-F females (Fig. 2.5C). From this, every individual per experiment was fit with a logistic model, and individuals with significant fits were noted (Table 2.4). Among significant individuals, a mean irradiance threshold of 1.74 x 10^9 photons $cm^{-2}s^{-1}$ was calculated for MS-S individuals (n = 30), 1.78 x 10^8 photons $cm^{-2}s^{-1}$ for PN-S (n = 7), and 4.47 x 10^8 photons $cm^{-2}s^{-1}$ in PN-F females (n = 21). Comparing each individual's thresholds across experimental trials, significant differences were observed between Midnight Sun and Polar Night groups. Irradiance threshold values were statistically higher among significant MS-S females (n = 30) compared to PN-F females (n = 21) (Kruskal-Wallis ANOVA, p = 0.019). While no significant differences are noted between MS-S and PN-S females (n = 7), median threshold is still higher in MS-S (3.47 x 10^9 photons $cm^{-2}s^{-1}$) vs. PN-S individuals (5.09 x 10^8 photons $cm^{-2}s^{-1}$) (Fig 2.6A).

Table 2.2: Significant Spectral Response Results. Significant p values (Holm-Bonferroni adjustment method, $p < 0.05$) greater than the average dark control are listed in bold per relevant wavelength.

Wavelength (nm)	Midnight Sun Female Spectral Response (MS-S)	Polar Night Female Spectral Response (PN-S + PN-F)	PN-S Female Spectral Response	PN-S CV Spectral Response
400	**0.048**	**3.09×10^{-6}**	0.051	0.84
430	0.120	**8.22×10^{-4}**	0.05	1
460	**3.87×10^{-6}**	**8.76×10^{-8}**	**0.021**	0.51
490	**9.09×10^{-7}**	**2.84×10^{-7}**	0.164	**0.004**
520	**1.45×10^{-8}**	**3.28×10^{-6}**	0.16	1
550	**0.007**	**0.036**	0.882	1
580	0.782	0.358	0.085	1
610	0.782	0.408	0.985	1
640	0.771	0.408	0.808	1
670	0.049	0.408	0.882	0.313

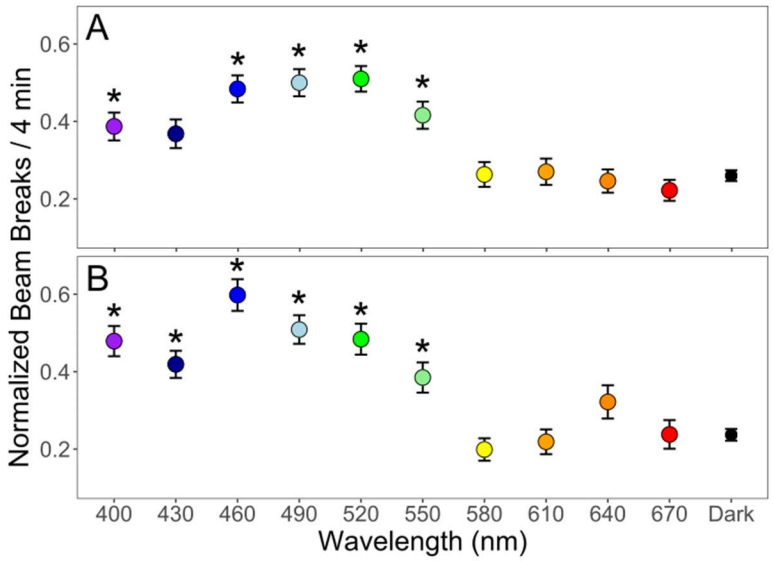

Figure 2.3: Spectral Response during Midnight Sun and Polar Night. Swimming response is plotted against wavelength for female *M. longa* tested during **(A)** Midnight Sun (MS-S) (n = 76), and **(B)** Polar Night (PN-S + PN-F) (n = 60). Circles represent the normalized means of each individual's beam break sums (± SE) per wavelength light stimulus (400 - 670 nm). The dark value (black) is a grand mean of each individual's mean response (± SE) during the dark periods before a wavelength exposure. Significant differences ($p < 0.05$) between swimming response during each light stimulus and the average dark control are noted using an asterisk (*). Differences were determined using a Friedman Test (non-parametric repeated measures ANOVA) with a paired Wilcoxon signed rank test.

Table 2.3: Significant Response Irradiance Results. Significant p values (Holm-Bonferroni adjustment method, $p < 0.05$) greater than the average dark control are listed in bold per relevant irradiance value.

Irradiance (photons $cm^{-2}s^{-1}$)	PN-S Female Irradiance Response	MS-S Female Irradiance Response	PN-S CV Irradiance Response	PN-F Female Irradiance Response	PN-F Daytime Female Irradiance Response	PN-F Nighttime Female Irradiance Response	PN-F 6°C Female Irradiance Response	PN-F -1°C Female Irradiance Response
2.7 - 2.93 x 10^5	0.65	1.00	0.68	0.63	1.00	1.00	1.00	1.00
8.55 - 9.27 x 10^5	1.00	0.44	1.00	1.00	1.00	1.00	1.00	1.00
2.7 - 2.93 x 10^6	1.00	1.00	1.00	0.95	1.00	1.00	1.00	1.00
8.55 - 9.27 x 10^6	1.00	0.52	0.42	0.06	1.00	1.00	1.00	1.00
4.29 - 4.65 x 10^7	0.46	1.00	1.00	0.08	1.00	0.036	1.00	1.00
8.55 - 9.27 x 10^7	1.00	1.00	0.66	1.00	0.25	1.00	1.00	1.00
4.29 - 4.65 x 10^8	0.83	1.00	0.29	1.00	1.00	1.00	0.06	0.39
8.55 - 9.27 x 10^8	1.00	1.00	1.00	1.00	1.00	1.00	**0.048**	**0.003**
3.4 - 3.69 x 10^9	0.654	**1.93 x 10^{-6}**	0.676	0.51	1.00	1.00	**3.38 x 10^{-5}**	**4.45 x 10^{-6}**
8.55 - 9.27 x 10^9	0.234	**1.67 x 10^{-7}**	1.00	**0.037**	**0.024**	1.00	**9.49 x 10^{-6}**	**3.17 x 10^{-7}**
2.7 - 2.93 x 10^{10}	0.826	**5.62 x 10^{-9}**	1.00	**0.004**	**0.027**	1.00	**1.05 x 10^{-6}**	**1.79 x 10^{-6}**
8.55 - 9.27 x 10^{10}	0.654	**1.82 x 10^{-8}**	1.00	0.053	**0.005**	0.341	**4.94 x 10^{-6}**	**3.73 x 10^{-6}**

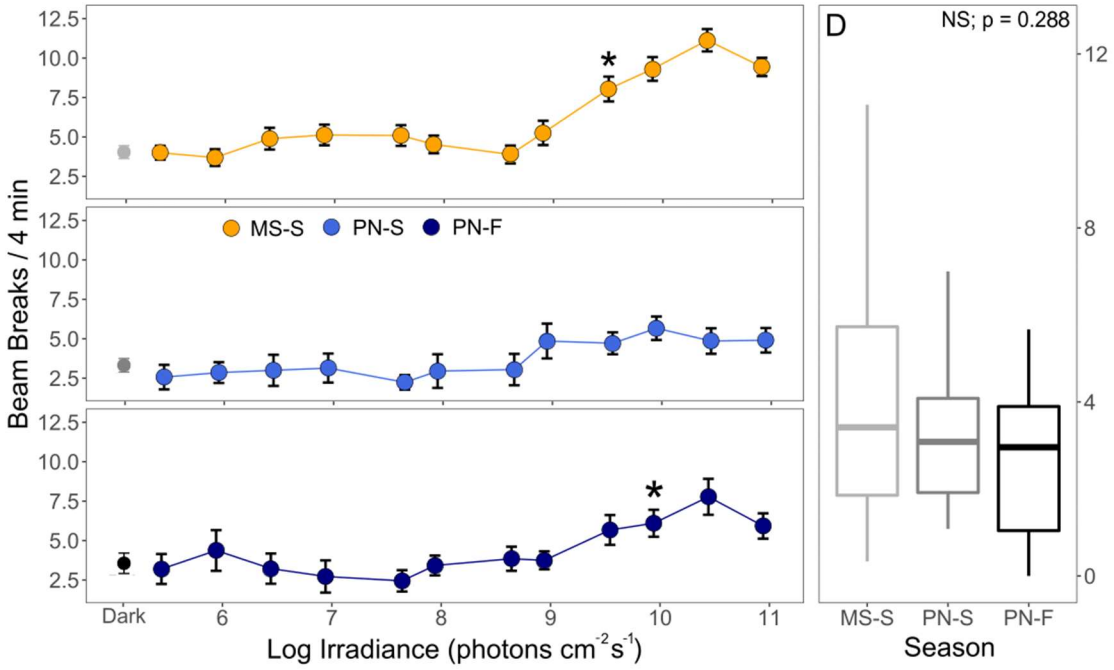

Figure 2.4: Irradiance Response during Midnight Sun and Polar Night. Swimming response is plotted against light intensity for female *M. longa* tested during Midnight Sun and Polar Night at **(A)** MS-S (n = 55)), **(B)** PN-S (n = 21), and **(C)** PN-F (n = 40) station. Points represent the means of each individual's beam break sums (± SE) per irradiance stimulus (2.7×10^5 - 9.27×10^{10} photons $cm^{-2}s^{-1}$). The dark value (black) is a grand mean of each individual's mean response (± SE) during the dark periods before an irradiance exposure. Significant differences ($p < 0.05$) between swimming response during each light stimulus and the average dark control are noted using an asterisks (*). Differences were determined using a Friedman Test (non-parametric repeated measures ANOVA) with a paired Wilcoxon signed rank test. (D) Boxplots represent activity during the dark portions of each experiment. Differences between each group's mean dark activity were determined using a non parametric one-way ANOVA (Kruskal-Wallis test).

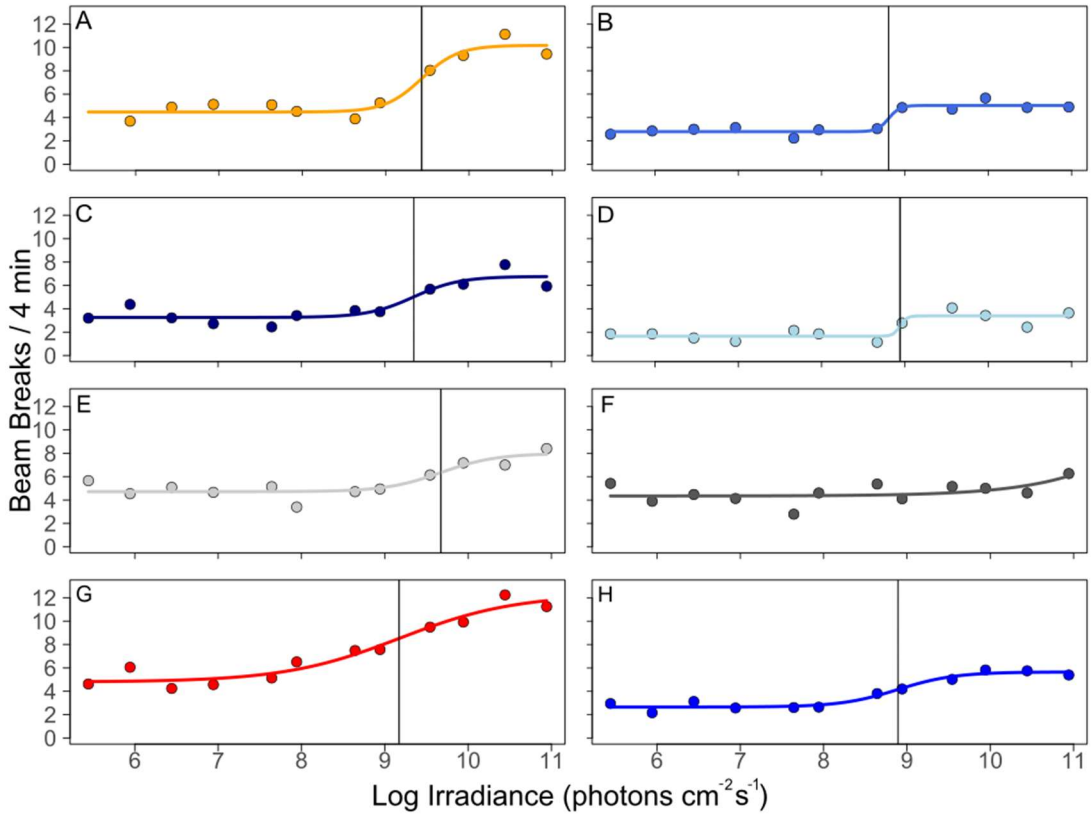

Figure 2.5: Sigmoid Logistic Dose-Response Curves per Irradiance Experiment. Mean swimming response is plotted against light intensity for M. longa females tested at the **(A)** MS-S, **(B)** PN-S, and **(C)** PN-F sampling stations. M. longa tested in Polar Night specific irradiance experiments are also plotted above, including **(D)** PN-S CV individuals, **(E)** Daytime females, **(F)** Nighttime females, **(G)** 6°C females, and **(H)** -1°C females. A description of point symbols is provided in Figure 2.4. Horizontal lines represent sigmoid 4-parameter logistic model fits for each irradiance experiment. Vertical black lines indicate estimated half-saturation, or irradiance thresholds, per trial.

Table 2.4: Significant Individuals per Response Irradiance Experiment via Logistic Dose-Response Model Analysis. Significant individuals (i.e. individuals whose swimming response could be fit with a significant model curve) per irradiance experimental trial are listed in the table below. The number of significant individuals per experiment are also compared to the total number of individuals previously analyzed (see Table 2.1 for details) and the proportion of significant to total individuals is included per experiment. Means of every significant individual's threshold value (± 95% confidence interval) were also calculated per experiment and reported below.

Station	Experiment	Significant Individuals (#)	Mean Threshold ± CI	Total Individuals (#)	% Significant
MS-S	Female Irradiance Response	30	9.24 ± 0.44	55	54%
PN-S	Female Irradiance Response	7	8.25 ± 1.23	21	33%
	CV Irradiance Response	5	9.57 ± 2.41	14	36%
PN-F	Female Irradiance Response	21	8.65 ± 0.47	40	53%
	Female Day Irradiance Response	15	8.25 ± 1.05	35	43%
	Female Night Irradiance Response	9	7.90 ± 1.59	38	24%
	Female 6°C Irradiance Response	21	8.66 ± 0.54	38	55%
	Female -1°C Irradiance Response	24	8.74 ± 0.65	56	43%

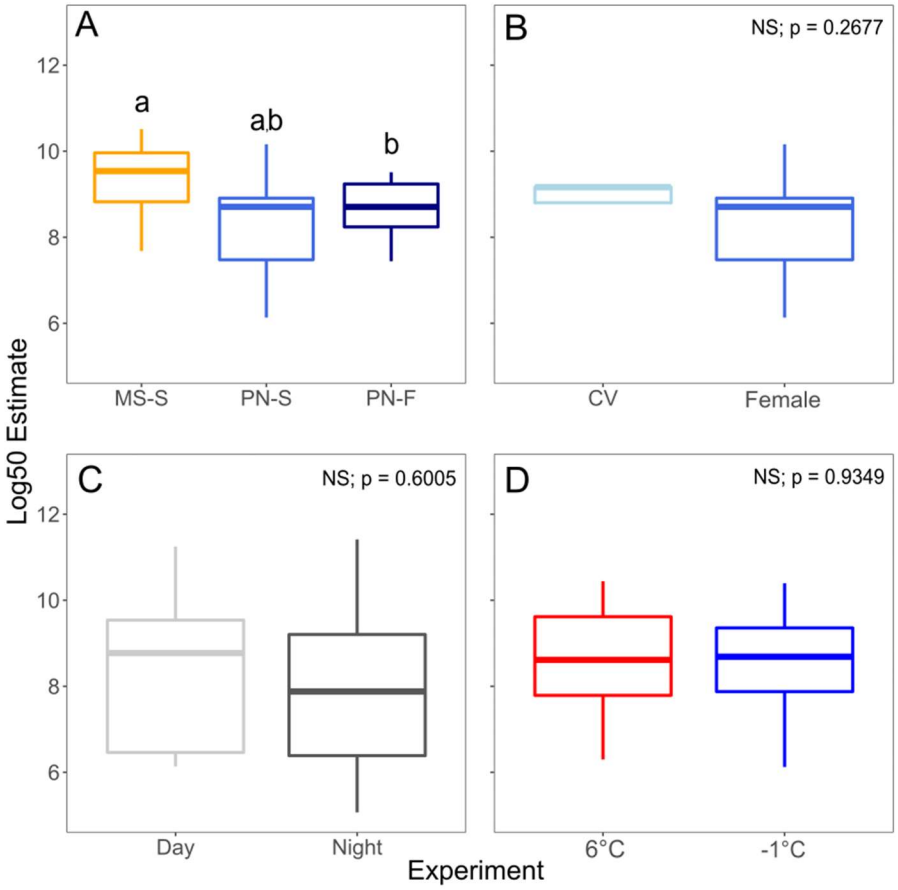

Figure 2.6: Comparison of Individual Irradiance Threshold Values per Experimental Trial. Estimated thresholds of significant individuals are compared between **(A)** Midnight Sun and Polar Night (MS-S, n = 30, vs. PN-S, n = 7, vs. PN-F, n = 21), **(B)** copepodite stage (PN-S CV, n = 5, vs. adult females, n = 7), **(C)** PN-F day (n = 15) and night (n = 9) irradiance experiments, and **(D)** temperature trials (PN-F 6°C, n = 21, vs -1°C, n = 24). Light period comparisons were analyzed using a non-parametric one-way ANOVA (Kruskal-Wallis test) with a post hoc Dunn's test and a Bonferroni p adjustment method, while other two factor comparisons were made with a non-parametric one-sample t-test (Wilcoxon test). Lowercase letters indicate statistically significant differences among individual threshold values between experimental trials.

2.3.3 Spectral and Irradiance Response During Polar Night: Stage, Time, and Temperature

Spectral and irradiance sensitivities were compared between copepodite stage V individuals (hereafter CV) (n = 17) and adult females (n = 20) at station PN-S. Both groups showed blue-green dominant light sensitivity. CV individuals and adult females showed increased swimming response above dark controls at 490 and 460 nm, respectively (Table 2.2) (Fig. 2.7A&B). Among sampled adult males at the PN-S station (n = 15), no significant spectral response above dark controls was found, but trends in elevated blue-green response as well as a longer wavelength response are observed (Fig. C1).

Both CV (n = 14) and adult female (n = 21) irradiance response at 490 nm results show no significant swimming response above dark controls. Just as in the females, a step increase in response may be present at 9.27×10^8 photons $cm^{-2}s^{-1}$ in CV individuals (Fig. 2.8A). This increase, however, is more prominent in female results (Fig. 2.8B). Females were also more active compared to CV individuals. The dark activity analysis showed median dark activity of 3.083 beam breaks / 48 min in females compared to 1.792 in CVs, and mean dark activity was significantly higher in females than CVs ($p = 0.037$). In tested adult males, an extremely low sample size was tested (n = 4) and no significant response above dark controls was found (Fig. C2).

In the logistic dose-response analysis, all CV PN-S individuals showed elevated mean response past 9.55×10^8 photons $cm^{-2}s^{-1}$ (Fig. 2.5D), slightly higher compared to the estimated threshold for adult PN-S females, 6.37×10^8 photons $cm^{-2}s^{-1}$ (Fig. 2.5B). Mean thresholds calculated only using significant individuals, however, show a higher irradiance threshold value by an order of magnitude in CV individuals (n = 5) vs. adult females (n = 7) (3.72×10^9 vs. 1.78×10^8 photons $cm^{-2}s^{-1}$

respectively) (Table 2.4). When comparing all significant CV and adult female individual's thresholds, median irradiance response was also higher in CV copepods (1.45×10^9 photons $cm^{-2}s^{-1}$) than adult females (5.09×10^8 photons $cm^{-2}s^{-1}$) (Fig. 2.6B).

PN-F females were tested for differences in irradiance response during the day and nighttime periods. Both irradiance experiments took place within 24 hours of sampling to ensure, if a diel rhythm was present, response wouldn't be lost to continued laboratory dark acclimation. Day females (n = 35) showed an irradiance threshold of 8.76×10^9 photons $cm^{-2}s^{-1}$ using the repeated measures statistical design (Table 2.3) (Fig. 2.9A). Night females, however, showed no significant movement above their average dark control throughout the entire experiment (Fig. 2.9B). Additionally, median baseline dark activity is higher in daytime individuals (4.5 beam breaks / 48 min) compared to nighttime individuals (3.833 beam breaks / 48 min) (Fig. 2.9C).

Similar results were noted when using the logistic dose-response method on the mean response across all individuals tested. In the daytime experiment, PN-F individuals showed increased response past 4.71×10^9 photons $cm^{-2}s^{-1}$ (Fig. 2.5E), whereas PN-F females tested at night still showed no significant response (Fig. 2.5F). However, among significant nighttime individuals (n = 9), irradiance response was potentially heightened compared to the significant individuals tested during the day (n = 15), responding to a mean value of 7.94×10^7 photons $cm^{-2}s^{-1}$ vs. 1.78×10^8 photons $cm^{-2}s^{-1}$ (Table 2.4). Significant night individuals also showed a lower median irradiance threshold, 7.59×10^7 photons $cm^{-2}s^{-1}$, compared to the significant individuals tested in the daytime experiment, 5.89×10^8 photons $cm^{-2}s^{-1}$ (Fig. 2.6C).

Temperature irradiance experiments tested *M. longa* females' acute light response at 6°C (n = 38) and -1°C (n = 56). Females tested at both temperatures show an irradiance threshold of 8.76 x 10^8 photons $cm^{-2}s^{-1}$ under the repeated measures analysis (Table 2.3) (Fig. 2.10). 6°C females, however, showed significantly higher photoresponse and dark activity (t-test, p = 7.515 x 10^{-7}) (inset plot on Fig. 2.10) compared to -1°C females. Additionally, photoresponse at irradiance threshold was significantly higher at 6°C than -1°C (p = 0.005817).

Logistic model results further validate consistency of irradiance response between temperatures. Mean response across all individuals was elevated past 5.50 x 10^8 photons $cm^{-2}s^{-1}$ at -1°C compared to 4.57 x 10^8 photons $cm^{-2}s^{-1}$ at 6°C (Fig 2.5G&H). Mean and median threshold values among significant individuals were also similar (mean: 4.57 vs. 5.50 x 10^8 photons $cm^{-2}s^{-1}$, median: 4.07 vs. 5.13 x 10^8 photons $cm^{-2}s^{-1}$ for -1 and 6°C respectively) (Fig 2.6D).

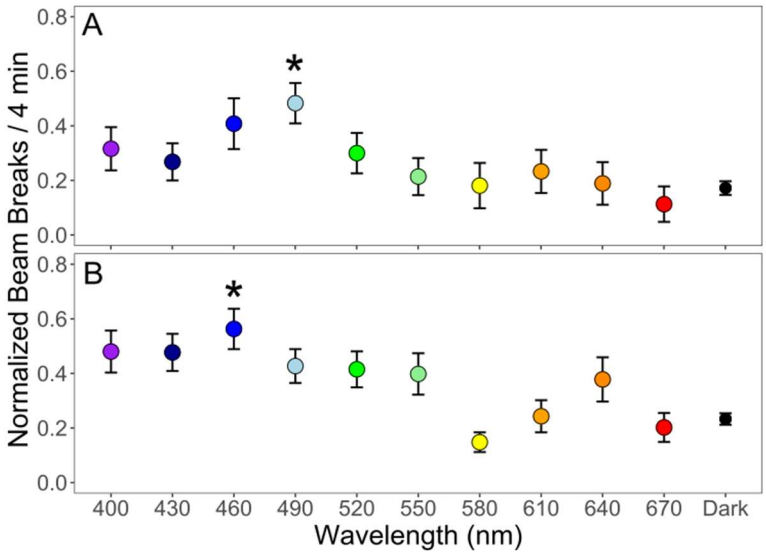

Figure 2.7: Spectral Response Across Copepodite Stages during Polar Night. Swimming response is plotted against wavelength for **(A)** CV (n = 17) and **(B)** adult female (n = 20) *M. longa* tested at the PN-S station. A further description of plot symbols and measures can be found in Figure 2.3.

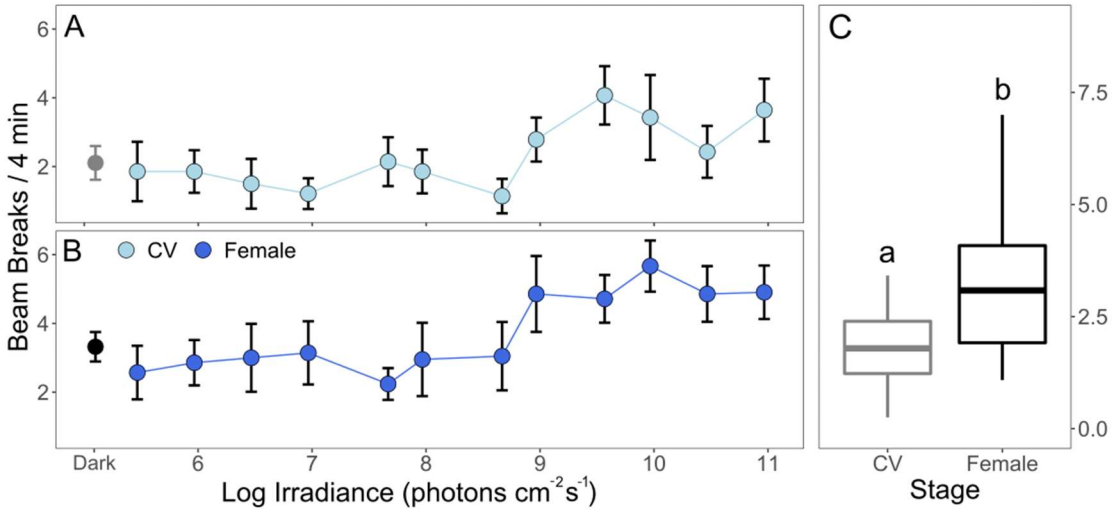

Figure 2.8: PN-S Irradiance Response Across Copepodite Stages during Polar Night. Swimming response is plotted against irradiance values (2.93 x 10^5 - 9.27 x 10^{10} photons $cm^{-2}s^{-1}$) for **(A)** CV (n = 14) and **(B)** adult female (n = 21) *M. longa* tested at the PN-S station. A further description of plot symbols and measures can be found in Figure 2.4. **(C)** The dark activity analysis, analyzed using a Wilcoxon rank sums test, revealed females were significantly more active than CV individuals (p = 0.036, indicated by lowercase letters).

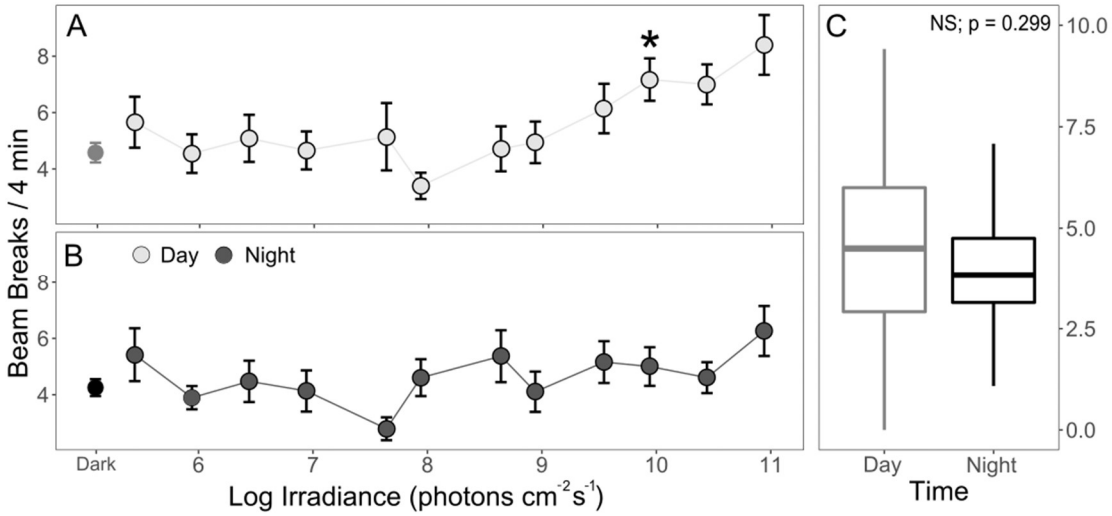

Figure 2.9: Irradiance Response between Day and Night during Polar Night. Swimming response is plotted against irradiance values (2.77×10^5 - 8.76×10^{10} photons $cm^{-2}s^{-1}$) for females tested during the **(A)** day (n = 35) and **(B)** night (n = 38) at the PN-F station. A further description of plot symbols and measures can be found in Figure 2.4. **(C)** Activity differences were quantified using a Wilcoxon rank sums test.

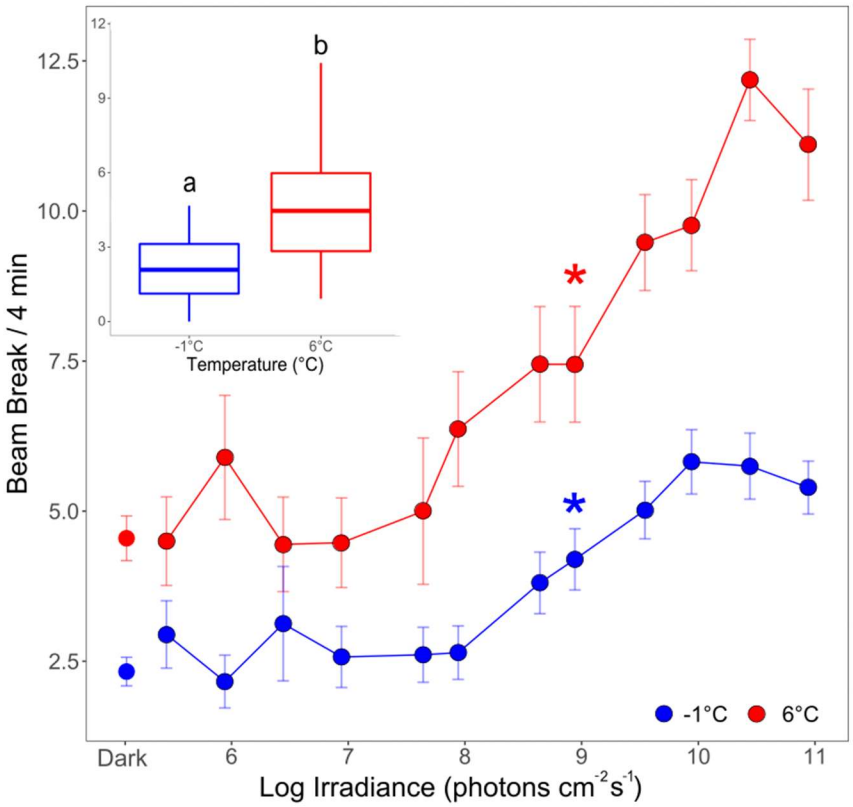

Figure 2.10: Irradiance Response between Temperatures during Polar Night. Swimming response is plotted against irradiance values (2.77×10^{5} - 8.76 x 10- photons $cm^{-2}s^{-1}$) for females tested at 6 °C (red) (n = 35) and -1°C (blue) (n = 56) at the PN-F station. A further description of the main and inset plot symbols and measures can be found in Figure 2.4. The dark activity analysis, analyzed using a Wilcoxon rank sums test, revealed females tested at 6°C were significantly more active than females at -1°C ($p = 7.515 \times 10^{-7}$, indicated by lowercase letters).

2.4 Discussion

Given the marked differences in light climate across the year at high latitudes, the objective of this study was to determine the behavioral responses of *M. longa* copepods to spectral and irradiance light stimuli during Midnight Sun and Polar Night in the high Arctic. Light sensitivity was also quantified during the Polar Night period between different copepod stages (CVs and adult females), locations (shelf vs. fjord), time of day (day vs. night) and temperature (-1°C vs. 6 °C). Overall, results suggest continuous blue-green dominant spectral response between Midnight Sun and Polar Night, and the potential for an increased irradiance response among Polar Night copepods compared to those tested during Midnight Sun. Additionally, irradiance response among *M. longa* copepods may vary with developmental stage, but are not dependent on location or temperature during the Polar Night season.

2.4.1 Spectral Response

Oceanic zooplankton, specifically vertical migrators that use the solar irradiance available at twilight as an external cue for migration, typically show a spectral sensitivity to blue-green wavelengths (Cohen and Forward, 2009, Cohen & Forward, 2002). This is consistent with the determined spectral response of *M. longa* females during Midnight Sun and Polar Night, which showed elevated swimming response from 400 to 550 nm during both light periods (Fig. 2.3). Increased activity in response to blue-green light also matches the results reported in Buskey and Swift (1985), who sampled *M. longa* off the coast of Iceland during summer and found elevated responses to wavelength flashes ranging from 460 to 560 nm. Blue-green sensitivity is also the case for the known spectral sensitivities of other major migratory Arctic zooplankton, including *Calanus* spp. copepods (C. *finmarchicus and C.*

glacialis) (Båtnes et al., 2013) and euphausiids (*Thysanoessa inermis* and *Meganyctiphanes norvegica,* λ_{max} = 490 nm) (Frank & Widder, 1999, Cohen et al., 2015a). In more tropical regions, studies on highly migratory zooplankton such as *Pleuromamma* spp. copepods reveal increased sensitivity at 480 nm (Buskey et al., 1989). Concerning Midnight Sun vs. Polar Night light sensitivity, I postulate that *M. longa* adult female spectral response is broad enough to account for the spectral changes between the two light periods. Early spring phytoplankton blooms and CDOM/suspended particulate matter peak absorbance is in the blue wavelengths, with exponential decays in absorbance through the green wavelengths, impacting the spectral light availability with depth towards green light during Midnight Sun (Grant et. al 2023, Castellani et al., 2022; Siegel et al., 2002). In contrast, Polar Night spectral irradiance is shifted toward blue light availability; spectral output of lunar irradiance peaks in the blue wavelengths (Cohen et al., 2020). Additionally, models show blue light propagation through the water column during Polar Night, an emissions peak of 485 nm available at depths beyond 30 m (Cohen et al., 2015a). *Metridia longa* copepods respond to wavelengths across blue-green light, helping them acclimatize to the annual changes of the Arctic light climate.

An ontogenetic difference in spectral response was not observed for *M. longa* copepods in this study. Both CV copepods and adult females showed a blue dominant sensitivity, with trends indicating extended green light sensitivity in adult females (Fig. 2.7). Båtnes et al. (2013) found a similar result among *Calanus* spp. copepodite stages, observing that spectral sensitivity tends to stay consistent across developmental stages. The same was found among *Rhithropanopeus harrisii* crab larvae (Forward & Costlow, 1974). Conversely, research on the instar phases of the freshwater insect

Chaoborus punctipennis found that spectral sensitivity changes throughout development, animals losing red sensitivity through instar changes as their environment shifts from shallow freshwater environment to air (Swift & Forward, 1980, 1982). Ecologically speaking, however, CV copepods and adult females are the dominant vertically migratory stages, adult males and younger stages remaining at depth despite external irradiance cues (Daase et al., 2008). Therefore, it stands to reason the two stages would exhibit a similar spectral light response sensitivity.

Blue-green spectral sensitivity is not only useful for vertical migration strategies in *M. longa* copepods, but may also aid bioluminescent light detection. Bioluminescent spectral emissions among marine species is often found in the blue-green wavelengths (Herring, 1988; Widder et al., 1983), and reported luminescence among copepods shows an emission range between 430 and 490 nm (Herring, 1983). Another northern *Metridia* species, *Metridia lucens*, for example, the bioluminescent emission spectrum peaked at 482 nm (David & Conover, 1961; Herring, 1983). Ecologically, research in Kongsfjorden during Polar Night has shown that *M. longa* copepods are a major contributor to bioluminescent light, particularly at increasing depth (Cronin et al., 2016). Buskey and Swift (1985) suggested that a visual sensitivity to blue-green light in *M. longa* could aid in predator avoidance strategies through warning flashes. The increased behavioral responses of *M. longa* females across 400 to 550 nm in this study is, therefore, consistent with both the spectral emissions of downwelling irradiance across seasons in the high Arctic, as well as bioluminescent light and light detection at depth.

2.4.2 Irradiance Response

Swimming activity was highly variable among *M. longa* copepods tested between Midnight Sun and Polar Night. During Midnight Sun, shelf (MS-S) females showed high photoresponse across the increasing intensity stimuli. Ecologically, calanoid copepods typically undergo diapause in winter seasons to reserve energy stores for springtime spawning and gonad development, an example being Arctic *Calanus* spp. who are energetically constrained to springtime phytoplankton blooms (Daase et al., 2008; Grigor et al., 2022). While *M. longa* copepods are omnivorous and remain active in the winter, they are still less metabolically active and rely partially on lipid reserves for energy (Hopkins et al., 1984). Across Polar Night experiments, significant dark activity differences were observed between copepodite stages and temperature. While temperature - activity implication will be discussed in relation to Arctic warming, differences in stage activity may suggest ontogenetic differences in ecological priorities (i.e. mating, molting, feeding, etc.).

Between Polar Night locations, photoresponse was elevated in fjord females (PN-F) compared to shelf copepods (PN-S). A potential higher photoresponse activity among fjord copepods compared to shelf is consistent with previous research on the swimming activity of *Calanus finmarchicus* across the shelf break in the Fram Strait in shallow vs. deep water basins. Grigor et al. (2022) found that copepods showed increased activity in the shallower shelf(~ 200 m depth) compared to the deeper basin (~2000 m depth).

Other potential activity differences exist during the day vs. night. Female *M. longa* exhibited higher median dark activity rates and photoresponse during the day, compared to females tested at night. This contradicts expectations concerning *M. longa* DVM patterns, animals moving to the surface at night and exhibiting stronger

activity. One plausible explanation is included in Gaten et al., (2008) in which Antarctic krill, *E. superba*, movement in a similar LAM system was recorded using top and bottom sensors, krill projected to show elevated response at the surface during the night and at the bottom of the test tube during the day. LAMs in this present study only contained one bottom sensor, a caveat discussed further in the experimental design section (2.4.4).

Overall, copepods showed less activity during Polar Night than Midnight Sun in both their photoresponse and median baseline dark movement (Fig. 2.4). Subsequently, while an increase in activity with irradiance was apparent during many Polar Night experiments, identifying irradiance thresholds based solely on the repeated measures statistical design was inconclusive, specifically in PN-S individuals. The comparison of continual low photoresponsiveness to baseline dark movement showed no significant results for this group. However, by conducting an individual based threshold analysis, using a logistic dose-response function to identify significant individuals in an experimental group, I was able to overcome the activity constraints associated with Arctic season and my experimental design.

I hypothesized that irradiance sensitivity would shift between the two times of year given their extreme differences in light climate (Cohen et. al, 2020) with *M. longa* females showing increased light sensitivity during Polar Night. Identified irradiance threshold values using the dose-response curve methodology differed by approximately one order of magnitude between Midnight Sun and Polar Night (10^9 vs. 10^8 photons $cm^{-2}s^{-1}$ respectively). These values correspond with the difference in available irradiance between the light periods, just below surface measurements in May and June documented in this study differing by five orders of magnitude (10^{16} vs.

10^{10} photons $cm^{-2}s^{-1}$) and are consistent with research showing that visual sensitivity increases in low light conditions. Viljanen et al. (2017), for example, reported photoreceptor damage among crustacean visual systems when readily exposed to increased light levels. Even on a diel scale, morphological shifts in eye sensitivity have been reported in *Tigriopus calfornicus* copepods, in which the photoreceptor membrane and visual pigments are synthesized in the dark (Martin et al., 2000).

Other studies have behaviorally quantified the irradiance sensitivity thresholds for other vertically migratory zooplankton species, a comprehensive list provided in Table 2.5. In a closely related environment during Polar Night, i.e. Arctic fjord, adult female and CV *Calanus* spp. showed elevated activity beyond 10^6 - 10^7 photons cm^{-2} s^{-1} at 455 nm (Båtnes et al., 2013). This is relatively similar to this study's modeled *M. longa* threshold in the Barents Sea during Polar Night (5.86 x 10^7 photons cm^{-2} s^{-1}), but more sensitive in comparison to the sampled fjord copepods (2.16 - 8.76 x 10^9 photons cm^{-2} s^{-1}). *Acartia tonsa* copepods sampled in a shallow turbid environment, i.e. a coastal estuary, also showed increased response past 10^7 photons cm^{-2} s^{-1} at 564 nm (Stearns & Forward, 1984). Deep oceanic *Pleuromamma c*opepods in the Sargasso Sea, *P. xiphias and P. gracilis* showed irradiance response threshold values of 10^6 - 10^8 photons cm^{-2} s^{-1} respectively (Buskey et al., 1989).

Specifically, Buskey & Swift (1985) quantified irradiance responses of *M. longa* individuals at 475 nm. In their study, *M. longa* copepods showed the highest mean swimming response, measured as speed, in response to 1.2 x 10^{12} photons cm^{-2} s^{-1} (value converted from µmol photons cm^{-2} s^{-1}, applicable to all subsequent values listed). However, mean swimming speed was already high at the lowest intensity exposure, 1.2 x 10^{11} photons cm^{-2} s^{-1} (Buskey & Swift, 1985). In the present study, *M.*

longa females were exposed to intensities ranging from 10^5 to 10^{10} photons cm^{-2} s^{-1} at 490 nm, which was lower in comparison to those quantified in Buskey & Swift (1985), and lower irradiance response thresholds were subsequently identified.

Attenuation coefficients calculated via $E_{d,PAR}$ measurements at each location, Barents Sea Shelf and Kongsfjorden, reveal clearer water conditions in the fjord during Polar Night as compared to the offshore shelf during Midnight Sun. In these measured environments under these two distinct light periods, using the lowest quantified irradiance thresholds in this study, *M. longa* copepods can detect light down to 55 m during the Polar Night in the fjord environment, while shelf animals can detect light to 119 m at midday during Midnight Sun. These depths correlate with the known depth ranges of copepods between both periods, zooplankton found closer to the surface during Polar Night and deeper in Midnight Sun due to isolume shifts. Hobbs et al. (2021), assuming an isolume intensity of 10^6 photons $cm^{-2}s^{-1}$, chosen as a midpoint known intensity threshold value for Arctic copepods and krill, found that zooplankton in Kongsfjorden remain in the top 100 m of the water column during Polar Night, only migrating approximately 10 m daily and remaining below an isolume depth of 21 - 23m. In Midnight Sun, conversely, zooplankton were pushed to greater depths with increased illumination moving the isolume downward in the water column. Center of zooplankton biomass was on average 120 m at midday from April through June. (Hobbs et al., 2021).

Additionally, using the maximum luminescence intensity reported in Clarke et al. (1962) for *M. longa* copepods, 2.97×10^8 photons cm^{-2} s^{-1}, I determined the detection range of bioluminescence in the water column during Polar Night for *M. longa* females. This value is an order of magnitude lower than the identified irradiance

response thresholds during Midnight Sun, but could be considered detectable light in Polar Night individuals. The lowest quantified Polar Night thresholds in this study, calculated as the half saturation of the dose-response curve among significant individuals, were within 10^8 photons cm^{-2} s^{-1}, but slightly higher or just at the reported bioluminescent intensity emitted by *M. longa* copepods. This suggests that *M. longa* luminescence may not be sufficient for conspecific detection. However, the variability of irradiance thresholds and light sensitivity per individual among fjord copepods indicates detection by some individuals over others. Additionally, reported intensities of bioluminescent ctenophores in Kongsfjorden, specifically *Beroe cucumis*, are two to three orders of magnitude higher than *M. longa* luminescence, indicating that *M. longa* irradiance thresholds may be useful for detection of co-occurring species (Cronin et al., 2016).

During Polar Night, CV and adult female copepods exhibited relatively similar sensitivity trends in the repeated measures analysis (Fig. 2.8B & D). In this case, a possible step increase in response was present at 10^8 photons $cm^{-2}s^{-1}$. In the dose-response model, however, females showed a lower irradiance threshold response by an order of magnitude in comparison to CV copepods (10^8 vs 10^9 photons cm^{-2} s^{-1}). While differences in individual thresholds were not significant, a lower irradiance response among adults is consistent with previous research documenting irradiance sensitivity differences across copepodite stages during Polar Night. For example, Båtnes et al. (2013) quantified irradiance response of *Calanus* spp. to blue green light, finding that adult females were more sensitive than CV copepods by two orders of magnitude (3.01×10^6 vs. 2.59×10^8 photons cm^{-2} s^{-1}). Additionally, studies suggest different opsin expression levels across developmental stages of *C. finmarchicus* copepods

(Porter et al., 2017). Cohen et al. (2015b) found that phototactic response to increasing intensities at 488 nm in *Hemigrapsus sanguineus* crab larvae changed across developmental stages, Z3 and Z5 zoea showing significant irradiance thresholds in comparison to Z1 individuals who showed little response. While results may indicate an ontogenetic difference in irradiance response present among *M. longa* copepodite stages, more data and further testing is needed for conclusive evidence.

Diel differences in irradiance response were quantified during Polar Night in this study, and results indicate that *M. longa* females show more pronounced photoresponse during the day compared to night (Fig 2.5 E&F, Fig. 2.9). The quantified irradiance thresholds for significant daytime individuals was within 10^8 to 10^9 photons $cm^{-2}s^{-1}$. In the repeated measures analysis, no elevated swimming response in relation to increasing light intensity was found in females tested during the subjective night period. These results contrast previous findings on light sensitivity changes during the day and night. Cohen et al. (2021), for example, reports diel sensitivity differences among *T. inermis* individuals in the Polar Night, ERG profiles showing an elevated irradiance sensitivity during the subjective nighttime vs. daytime. Increased nighttime sensitivity is also reported in other Arctic and Antarctic euphausiids (Gaten et al., 2008) as well as *Calanopia americana* copepods (Cohen & Forward, 2005). However, in the dose-response analysis, mean thresholds among nighttime individuals were an order of magnitude lower than the lowest threshold quantified in daytime individuals (10^7 vs. 10^8 photons $cm^{-2}s^{-1}$). While this is consistent with a heightened nighttime irradiance sensitivity, more conclusive evidence and increased sampling/testing of active nighttime individuals is needed to confirm day vs. nighttime light response results in *M. longa* copepods. Additionally, response results

could be solved through the use of additional LAM sensor plates, detailed above as a solution to day vs. nighttime activity results, as well as further mentioned in the experimental design caveats section below (2.4.4)

Across temperature treatments, *M. longa* females showed no significant differences in irradiance response (Fig 2.5G & H, Fig. 2.10). Research on vision in relation to temperature found that, in higher temperatures, visual systems can become faster (Cohen & Frank, 2006), but overall less sensitive to changes in irradiance (Frank, 2003; Tatler et al., 2000). Results from the logistic model may indicate decreased sensitivity among significant individuals tested at 6°C compared to -1°C. At 6°C, increased response occurs at 2.6×10^{9} photons $cm^{-2}s^{-1}$, while at -1°C, activity increases past 4.98×10^{8} photons $cm^{-2}s^{-1}$. However, median thresholds among significant individuals are approximately the same, and no significant differences were found when comparing treatments in this manner. Cohen & Frank (2006) found increased visual speed in a deep-sea Antarctic amphipod, *Abyssorchomene plebs*, with increased temperature, but noted no changes to irradiance sensitivity when compared between 3°C and 7°C. Since they are active vertical migrators, *M. longa* copepods experience vertical shifts in temperature on a daily basis. From CTD profiles taken in this study, temperature gradients across the sampled 300 m can vary by a magnitude of 0.76 to 0.96°C during Polar Night (PN-S and PN-F temperature gradients specifically) and 0.75°C during Midnight Sun (MS-S). *Metridia longa* females experience this vertical temperature variability daily based on their environment, and seem to be equipped to maintain light sensitivity in lieu of vertical and seasonal temperature differences.

Table 2.5: Reported irradiance threshold values among other zooplankton species. Irradiance sensitivity values reported for copepods, including the *M. longa* tested in this study, euphausiids, and amphipods are listed along with relevant stages of animals tested. Also included are the methods by which thresholds were determined (behavioral vs. electroretinogram) and experimental parameters, including the wavelength and duration of the light stimulus. Reported threshold values per study were converted into photons $cm^{-2}s^{-1}$ from µmol photons $cm^{-2}s^{-1}$ by converting µmol to mol (dividing by $1x10^{-6}$) and multiplying mol photons $cm^{-2}s^{-1}$ by Avogadro's number (6.022×10^{23}). The conversion between photons $m^{-2}s^{-1}$ and photons $cm^{-2}s^{-1}$ were made by dividing by $1x10^{4}$. Relevant literature is cited in the reference column.

Species	Location	Method	Experimental Temperature (°C)	Stage	Light Stimulus (s)	Wavelength (nm)	FWHM (nm)	Irradiance Threshold (photons $cm^{-2}s^{-1}$)	Reference
Metridia longa	Barents Sea Atlantic Shelf, Kongsfjorden	Behavioral	Seasonal 2°C - 3°C	Adult Females	2, 60 s flashes per intensity	490	10	Midnight Sun (MS-S): **10^9** Polar Night (PN-S&F): **10^8**	Present Study
			3°C	CV	2, 60 s flashes per intensity	490	10	PN-S: **10^9**	Present Study
Copepods									
Metridia longa	Iceland	Behavioral	2-6°C		60 ms	475		1.0 x **10^{12}**	Buskey & Swift, 1985
Acartia tonsa	Newport River Estuary, North Carolina	Behavioral	21-23°C	Adult Females	75 s	564		2.80 x **10^7**	Sterns & Forward, 1984
Calanopia americana	Newport River Estuary, North Carolina	Behavioral	23°C	Adult Females	5 min	Blue-green spectrum		↑ Intensities: **10^7**	Cohen & Forward, 2005
Calanus spp.	Adventfjorden, Svalbard	Behavioral	1 - 2°C	CV; Adult Females		455	23	3.07 x 10^7;3.01 x **10^6**	Båtnes et al., 2013
		Behavioral		CV: Adult Female		525	27	2.05 x **10^7;** 1.02 x **10^7**	Båtnes et al., 2013
Pleuromamma gracilis	Sargasso Sea	Behavioral	15°C	Adults		480		9.5 x **10^8**	Buskey et al., 1989
Pleuromamma xiphias	Sargasso Sea	Behavioral		Adults		480		7.7 x **10^6**	Buskey et al., 1989
Euphausiid									
Meganyctiphanes norvegica	Wilkinson Basin	Behavioral	7°C		10 s	500	50	**10^7**	Myslinski et al., 2005
	Wilkinson Basin (WB) & Oceanographer Canyon (OC)	ERG			100 ms	480		WB: **10^{11}** OC:**10^{12}**	Myslinski et al., 2005
Amphipod									
Abyssorchomene plebs	McMurdo Sound, Antarctica	ERG	3°C		75 ms	480 - 490	15	4.68 x **10^{12}**	Cohen & Frank, 2006
		ERG	7°C		76 ms	481 - 490	15	5.01 x **10^{12}**	Cohen & Frank, 2006

2.4.3 Climate Change and the Implications for Zooplankton Populations

The Arctic is rapidly experiencing the effects of climate induced change, increasing atmospheric temperatures exponentially decreasing sea ice extent, and the "Atlantification", or Atlantic water mass conditions extending towards Arctic waters, rapidly warming the region's oceans (Asbjørnsen et al., 2020; Tesi et al., 2021). While irradiance response was found to be independent of temperature among *M. longa* females, activity was significantly increased at 6°C vs. -1°C. This holds implications for *M. longa* metabolic activity in a warming Arctic environment. Between these temperature ranges, *M. longa* females have a Q_{10} value of 2.16, which is typical for biochemical reactions (Somero et. al, 2017). In areas such as the Fram Strait, the increased presence of warm, well mixed Atlantic waters has been found to increase *C. finmarchicus* developmental rates and aid in their overwintering strategies, shifts in algal blooms causing increased energy intake for survival of increasingly shorter winters. However, this holds implications for energy transfer across Arctic food webs, warming conditions favoring smaller zooplankton with subsequently smaller lipid stores in comparison with larger copepods (Tarling et al., 2022). Similar findings could hold true for *M. longa* copepods. However, increased activity rates could mean more rapid use of lipid stores, *M. longa* remaining more active in winter months compared to Calanus, as well as increased interactions with light, leading to further interactions with predators as well as changes to visual sensitivity (Varpe et al., 2015).

With the continual loss of sea ice, recent studies also predict downward bathymetric shifts in pelagic organism's distribution in the water column with increasing light and temperature. Such downward shifts are projected to further impact future predator-prey relations and overall light detection among zooplankton and fish

species. In this case, with increased temperatures and shifts in isolume depths being the driving factors, a narrower spectrum of available light at greater depths may affect marine animals in respect to their spectral response sensitivities (Caves & Johnsen, 2021). In this present study, irradiance response was unaffected by temperature, but spectral response may change with narrower availability at depth. Additionally, both may change in regard to greater illumination in the water column (Viljanen et al., 2017).

At greater depths, prey are theorized to have the advantage over visual predators in a darker environment, but at the expense of their foraging abilities (Caves & Johnsen, 2021). Varpe et al. (2015), however, projects increased trophic pressure on zooplankton communities, specifically larger zooplankton and copepods, theorizing that visual predators will be able to detect larger copepod prey at increased rates under the increased light conditions. This will in turn shift the available prey towards smaller zooplankton, impacting animals at higher trophic levels and the ecosystem as a whole. Loss of sea ice may also impact Midnight Sun copepod DVM behaviors, Wallace et al. (2010) characterizing DVM as intermittent under continued sea ice, but more asynchronized in open ocean conditions. Therefore, changes to the Arctic underwater light scape through climate-induced changes will negatively impact zooplankton populations, specifically in their light mediated processes and, therefore, foraging strategies, predator-prey relations, and trophic dynamics.

2.4.4 Experimental Design Novelty and Caveats

Overall, the apparatus used in this study is novel to the field of visual ecology. Previous behavioral methods have involves lower light resolution, using fewer wavelength and neutral density filters, lower individual resolution, and longer

experimental timeframes, continuous recordings of group behavior analyzed post experiment (Båtnes et al., 2015; Buskey et al., 1989; Buskey & Swift, 1985). Similar individualized behavioral light response methods, including those used in Kennedy et al. (2022), also allowing individual data collection and wavelength/intensity control, can only test six individuals at a time and relies on ice packs for temperature control since the system is bulky (experiments take place in an 18-gallon bin) (Kennedy et al., 2022). My experimental set-up allows simultaneous data collection for 64 individuals in one experiment (scalable to more), and can be used in walk-in or reach-in environmental chambers for more precise temperature control.

While the system allows for high throughput, individualized behavioral data collection, there are caveats to the design as a whole. For example, previous light sources have been brighter and, therefore, able to offer more light across spectral and irradiance experiments if needed (Buskey & Swift, 1985; Stearns & Forward, 1984). Additionally, the use of a monochromator, as in Cohen & Forward (2002), allows for increased resolution and finetuning of spectral light stimuli. The lack of continuous video recordings in this study also provided a knowledge gap as to what swimming behaviors animals executed in an experiment. Such recordings could explain the seemingly low beam break response among PN-S individuals, for example, and the sensitivity/activity differences between day and night PN-F females. Another solution, as mentioned earlier, could be more LAM sensor positions at the top and bottom of the test tubes. This, coupled with recordings of animal behavior, could provide a full picture to the behavioral light sensitivities of target zooplankton species.

2.5 Conclusion and Future Work

In this study, I used a newly developed, high throughput behavioral apparatus to quantify the spectral and irradiance sensitivities of the Arctic copepod *M. longa* across the two distinct light periods, Midnight Sun and Polar Night. I conclude that spectral sensitivity is continuously blue-green dominant across the photoperiods, allowing *M. longa* copepods to adapt to the changes in spectral output throughout the year (i.e. solar vs lunar spectral emission, spring phytoplankton blooms, CDOM, etc.). Irradiance response also seems to shift during the Polar Night in comparison to Midnight Sun. While low activity levels were pronounced during Polar Night, individualized logistic dose-response results showed increased sensitivity among PN-S and PN-F females compared to MS-S. During Polar Night, adult females and CV individuals exhibited similar spectral response trends, but an ontogenetic difference in irradiance response may be present between stages. Additionally, with respect to the seasonal variability of their habitat and vertical migration behavior, *M. longa* females are able to maintain visual sensitivity across varying temperatures. However, diel sensitivity results for *M. longa* may contrast other reports of increased nighttime sensitivity among zooplankton species, even in Polar Night conditions.

Data from this study can be used to focus logistically challenging electrophysiological ERG-based studies on *Metridia longa* copepods, as well as be paired with other physiological and molecular data to provide a full picture behind behavior and visual sensitivity in zooplankton species. For example, understanding the diel and seasonal variation in opsin expression could help explain these behavioral data. Future research should involve assessing the changes in *M. longa* sensitivity responses under a climate-change focus, simulating behavior in response to increased levels of light in the water column. Additionally, the behavioral apparatus used in this

study can be improved upon, the potential additions of more sensor plates at the tops of the test tubes, as well as the implementation of video recordings filling in knowledge gaps to zooplankton swimming behavior in experiments. This would be especially useful for gaining a conclusive understanding of developmental differences and diel changes in light sensitivity among *M. longa* copepods.

REFERENCES

Asbjørnsen, H., Årthun, M., Skagseth, Ø., & Eldevik, T. (2020). Mechanisms Underlying Recent Arctic Atlantification. *Geophysical Research Letters*, *47*(15), e2020GL088036. https://doi.org/10.1029/2020GL088036

Båmstedt, U., & Tande, K. (1988). Physiological responses of *Calanus finmarchicus* and *Metridia longa* (Copepoda: *Calanoida*) during the winter-spring transition. *Marine Biology*, *99*(1), 31–38. https://doi.org/10.1007/BF00644974

Båtnes, A. S., Miljeteig, C., Berge, J., Greenacre, M., & Johnsen, G. (2013). Quantifying the light sensitivity of *Calanus* spp. during the polar night: Potential for orchestrated migrations conducted by ambient light from the sun, moon, or aurora borealis? *Polar Biology*, *38*(1), 51–65. https://doi.org/10.1007/s00300-013-1415-4

Båtnes, A. S., Miljeteig, C., Berge, J., Greenacre, M., & Johnsen, G. (2015). Quantifying the light sensitivity of *Calanus* spp. during the polar night: Potential for orchestrated migrations conducted by ambient light from the sun, moon, or aurora borealis? *Polar Biology*, *38*(1), 51–65. https://doi.org/10.1007/s00300-013-1415-4

Berge, J., Cottier, F., Varpe, Ø., Renaud, P. E., Falk-Petersen, S., Kwasniewski, S., Griffiths, C., Søreide, J. E., Johnsen, G., Aubert, A., Bjærke, O., Hovinen, J., Jung-Madsen, S., Tveit, M., & Majaneva, S. (2014). Arctic complexity: A case study on diel vertical migration of zooplankton. *Journal of Plankton Research*, *36*(5), 1279–1297. https://doi.org/10.1093/plankt/fbu059

Berge, J., Daase, M., Hobbs, L., Peterson, S.-F., Darnis, G., & Søreide, J. E. (2020a). Zooplankton in the Polar Night. In *Polar Night Marine Ecology: Light and Life in the Dead of Night*.

Berge, J., Johnsen, G., & Cohen, J. H. (2020b). Introduction. In *Polar Night Marine Ecology: Life and Light in the Dead of Night* (Vol. 4). Springer Nature Switzerland.

Buskey, E. J., Baker, K. S., Smith, R. C., & Swift, E. (1989). Photosensitivity of the oceanic copepods *Pleuromamma gracilis* and *Pleuromamma xiphias* and its relationship to light penetration and daytime depth distribution. *Marine Ecology Progress Series*, *55*(2/3), 207–216.

Buskey, E. J., & Swift, E. (1985). Behavioral Responses of Oceanic Zooplankton to Simulated Bioluminescence. *Bio Bull*, 263–275.

Castellani, G., Veyssière, G., Karcher, M., Stroeve, J., Banas, S. N., Bouman, A. H., Brierley, S. A., Connan, S., Cottier, F., Große, F., Hobbs, L., Katlein, C., Light, B., McKee, D., Orkney, A., Proud, R., & Schourup-Kristensen, V. (2022). Shine a light: Under-ice light and its ecological implications in a changing Arctic Ocean. *Ambio*, *51*(2), 307–317. https://doi.org/10.1007/s13280-021-01662-3

Caves, E. M., & Johnsen, S. (2021). The sensory impacts of climate change: Bathymetric shifts and visually mediated interactions in aquatic species. *Proceedings of the Royal Society B: Biological Sciences*, *288*(1949), 20210396. https://doi.org/10.1098/rspb.2021.0396

Clarke, G. L., Conover, R. J., David, C. N., & Nicol, J. a. C. (1962). Comparative studies of luminescence in copepods and other pelagic marine animals. *Journal of the Marine Biological Association of the United Kingdom*, *42*(3), 541–564. https://doi.org/10.1017/S0025315400054254

Cohen, J. H., Berge, J., Moline, M. A., Johnson, G., & Zolich, A. P. (2020). Light in the Polar Night. In *Polar Night Marine Ecology: Life and Light in the Dead of Night* (Vol. 4).

Cohen, J. H., Berge, J., Moline, M. A., Sørensen, A. J., Last, K., Falk-Petersen, S., Renaud, P. E., Leu, E. S., Grenvald, J., Cottier, F., Cronin, H., Menze, S., Norgren, P., Varpe, Ø., Daase, M., Darnis, G., & Johnsen, G. (2015a). Is Ambient Light during the High Arctic Polar Night Sufficient to Act as a Visual Cue for Zooplankton? *PLOS ONE*, *10*(6), e0126247. https://doi.org/10.1371/journal.pone.0126247

Cohen, J. H., & Forward, R. B. (2002). Spectral Sensitivity of Vertically Migrating Marine Copepods. *Biological Bulletin*, *203*(3), 307–314. https://doi.org/10.2307/1543573

Cohen, J. H., & Forward, R. B. (2005). Diel vertical migration of the marine copepod *Calanopia americana*. I. Twilight DVM and its relationship to the diel light cycle. *Marine Biology*, *147*(2), 387–398. https://doi.org/10.1007/s00227-005-1569-x

Cohen, J. H., & Frank, T. M. (2006). Visual Physiology of the Antarctic Amphipod *Abyssorchomene plebs*. *The Biological Bulletin*, *211*(2), 140–148. https://doi.org/10.2307/4134588

Cohen, J. H., Hanson, C. K., Dittel, A. I., Miller, D. C., & Tilburg, C. E. (2015b). The ontogeny of larval swimming behavior in the crab *Hemigrapsus sanguineus*: Implications for larval transport. *Journal of Experimental Marine Biology and Ecology*, *462*, 20–28. https://doi.org/10.1016/j.jembe.2014.10.003

Connan-McGinty, S., Banas, N. S., Berge, J., Cottier, F., Grant, S., Johnsen, G., Kopec, T. P., Porter, M., & McKee, D. (2022). Midnight Sun to Polar Night: A Model of Seasonal Light in the Barents Sea. *Journal of Advances in Modeling Earth Systems*, *14*(10), e2022MS003198. https://doi.org/10.1029/2022MS003198

Cronin, H. A., Cohen, J. H., Berge, J., Johnsen, G., & Moline, M. A. (2016). Bioluminescence as an ecological factor during high Arctic polar night. *Scientific Reports*, *6*(1), Article 1. https://doi.org/10.1038/srep36374

Daase, M., Eiane, K., Aksnes, D. L., & Vogedes, D. (2008). Vertical distribution of *Calanus* spp. and *Metridia longa* at four Arctic locations. *Marine Biology Research*, *4*(3), 193–207. https://doi.org/10.1080/17451000801907948

David, C. N., & Conover, R. J. (1961). Preliminary Investigation of the Physiology and Ecology of Luminescence in the Copepod, *Metridia lucens*. https://doi.org/10.2307/1539462

Forward, R. B., & Costlow, J. D. (1974). The ontogeny of phototaxis by larvae of the crab *Rhithropanopeus harrisii*. *Marine Biology*, *26*(1), 27–33. https://doi.org/10.1007/BF00389083

Frank, T. M. (2003). Effects of Light Adaptation on the Temporal Resolution of Deep-sea Crustaceans. *Integrative and Comparative Biology*, *43*(4), 559–570. https://doi.org/10.1093/icb/43.4.559

Frank, T. M., & Widder, E. A. (1999). Comparative study of the spectral sensitivities of mesopelagic crustaceans. *Journal of Comparative Physiology A*, *185*(3), 255–265. https://doi.org/10.1007/s003590050385

Gaten, E., Tarling, G., Dowse, H., Kyriacou, C., & Rosato, E. (2008). Is vertical migration in Antarctic krill (*Euphausia superba*) influenced by an underlying circadian rhythm? *Journal of Genetics*, *87*(5), 473–483. https://doi.org/10.1007/s12041-008-0070-y

Grant, S., G. Johnsen, D. McKee, A. Zolich, and J.H. Cohen (in press) Spectral and RGB analysis of the light climate and its ecological impacts using an all-sky camera system in the Arctic. *Applied Optics*.

Grigor, J. J., Freer, J., Tarling, G. A., Cohen, J. H., & Last, K. S. (2022). Swimming Activity as an Indicator of Seasonal Diapause in the copepod *Calanus finmarchicus*. *Frontiers in Marine Science*.

Häfker, N. S., McGinty, S. C., Hobbs, L., McKee, D., Cohen, J. H., Last, K. S. (2022). Animal Behavior is Central in Shaping the Realized Diel Light Niche. *Comm Bio*. https://doi.org/10.1038/s42003-022-03472-z.

Hancke, K., Hovland, E. K., Volent, Z., Pettersen, R., Johnsen, G., Moline, M. A., & Sakshaug, E. (2014). Optical properties of CDOM across the Polar Front in the Barents Sea: Origin, distribution and significance. *ScienceDirect*. https://www.sciencedirect.com/science/article/abs/pii/S0924796312001510?via%3Dihub

Herring, P. J. (1983). The Spectral Characteristics of Luminous Marine Organisms. *Proceedings of the Royal Society of London. Series B, Biological Sciences*, *220*(1219), 183–217.

Herring, P. J. (1988). Copepod luminescence. *Hydrobiologia*, *167*(1), 183–195. https://doi.org/10.1007/BF00026304

Hobbs, L., Banas, N. S., Cohen, J. H., Cottier, F. R., Berge, J., & Varpe, Ø. (2021). A marine zooplankton community vertically structured by light across diel to interannual timescales. *Biology Letters*, *17*(2), 20200810. https://doi.org/10.1098/rsbl.2020.0810

Hopkins, C. C. E., Tande, K. S., Grønvik, S., & Sargent, J. R. (1984). Ecological investigations of the zooplankton community of balsfjorden, Northern Norway: An analysis of growth and overwintering tactics in relation to niche and environment in *Metridia longa* (Lubbock), *Calanus finmarchicus* (Gunnerus), *Thysanoessa inermis* (Krøyer) and *T. raschi* (M. Sars). *Journal of Experimental Marine Biology and Ecology*, *82*(1), 77–99. https://doi.org/10.1016/0022-0981(84)90140-0

Johnsen, G., Zolich, A., Grant, S., Bjørgum, R., Cohen, J. H., McKee, D., Kopec, T. P., Vogedes, D., & Berge, J. (2021). All-sky camera system providing high temporal resolution annual time series of irradiance in the Arctic. *Applied Optics*, *60*(22), 6456–6468. https://doi.org/10.1364/AO.424871

Kennedy, M. D., Barberio, A., & Connaughton, V. P. (2022). Novel experimental apparatus for laboratory measurements of phototaxis: A comparison between amphipod species. *Journal of Crustacean Biology*, *42*(1), ruab085. https://doi.org/10.1093/jcbiol/ruab085

Kirk, J. (2010). Concepts of hydrologic optics. In *Light & Photosynthesis in Aquatic Systems* (2nd ed.). Cambridge University Press.

Klekowski, R. Z., Weslawski, J. M., Skakuj, M., Malinga, M., & Stempniewicz, L. (1991). *Atlas of the marine fauna of southern Spitsbergen. Vol. 2, part 1: Invertebrates* (Vol. 2).

Langbehn, T. J., & Varpe, Ø. (2017). Sea-ice loss boosts visual search: Fish foraging and changing pelagic interactions in polar oceans. *Global Change Biology*, *23*(12), 5318–5330. https://doi.org/10.1111/gcb.13797

Leu, E., Graeve, M., & Wulff, A. (2016). A (too) bright future? Arctic diatoms under radiation stress. *Polar Biology*, *39*(10), 1711–1724. https://doi.org/10.1007/s00300-016-2003-1

Martin, G. G., Speekmann, C., & Beidler, S. (2000). Photobehavior of the Harpacticoid Copepod *Tigriopus californicus* and the Fine Structure of Its Nauplius Eye. *Invertebrate Biology*, *119*(1), 110–124.

Mehner, T., & Kasprzak, P. (2011). Partial diel vertical migrations in pelagic fish. *Journal of Animal Ecology*, *80*(4), 761–770. https://doi.org/10.1111/j.1365-2656.2011.01823.x

Ogonowski, M., Duberg, J., Hansson, S., & Gorokhova, E. (2013). Behavioral, Ecological and Genetic Differentiation in an Open Environment—A Study of a Mysid Population in the Baltic Sea. *PLOS ONE*, *8*(3), e57210. https://doi.org/10.1371/journal.pone.0057210

Onarheim, I. H., & Årthun, M. (2017). Toward an ice-free Barents Sea. *Geophysical Research Letters*, *44*(16), 8387–8395. https://doi.org/10.1002/2017GL074304

Pavlov, A. K., Leu, E., Hanelt, D., Bartsch, I., Karsten, U., Hudson, S. R., Gallet, J.-C., Cottier, F., Cohen, J. H., Berge, J., Johnsen, G., Maturilli, M., Kowalczuk, P., Sagan, S., Meler, J., & Granskog, M. A. (2019). The Underwater Light Climate in Kongsfjorden and Its Ecological Implications. In H. Hop & C. Wiencke (Eds.), *The Ecosystem of Kongsfjorden, Svalbard* (pp. 137–170). Springer International Publishing. https://doi.org/10.1007/978-3-319-46425-1_5

Porter, M., Steck, M., Roncalli, V., & Lenz, P. H. (2017). Molecular Characterization of Copepod Photoreception. *Biological Bulletin,* 233(1). https://doi.org/10.1086/694564

Reyes, B. A., Pendergast, J. S., & Yamazaki, S. (2008). Mammalian Peripheral Circadian Oscillators Are Temperature Compensated. *Journal of Biological Rhythms*, *23*(1), 95–98. https://doi.org/10.1177/0748730407311855

Siegel, D. A., Maritorena, S., Nelson, N. B., Hansell, D. A., & Lorenzi-Kayser, M. (2002). Global distribution and dynamics of colored dissolved and detrital organic materials. *Journal of Geophysical Research: Oceans*, *107*(C12), 21-1-21–14. https://doi.org/10.1029/2001JC000965

Somero, G. A., Lockwood, B. L., & Tomank, L. (2017). Biochemical Adaptation: Response to Environmental Challenges from Life's Origins to the Anthripocene.

Stearns, D. E., & Forward, R. B. (1984). Photosensitivity of the calanoid copepod *Acartia tonsa*. *Marine Biology*, *82*(1), 85–89. https://doi.org/10.1007/BF00392766

Swift, M. C., & Forward, R. B. (1980). Photoresponses of Chaoborus larvae. *Journal of Insect Physiology*, *26*(6), 365–371. https://doi.org/10.1016/0022-1910(80)90006-2

Swift, M. C., & Forward, R. B. (1982). Photoresponses of second-instar Chaoborus larvae. *Journal of Insect Physiology*, *28*(2), 183–187. https://doi.org/10.1016/0022-1910(82)90127-5

Tarling, G. A., Freer, J. J., Banas, N. S., Belcher, A., Blackwell, M., Castellani, C., Cook, K. B., Cottier, F. R., Daase, M., Johnson, M. L., Last, K. S., Lindeque, P. K., Mayor, D. J., Mitchell, E., Parry, H. E., Speirs, D. C., Stowasser, G., & Wootton, M. (2022). Can a key boreal *Calanus* copepod species now complete its life cycle in the Arctic? Evidence and implications for Arctic food-webs. *Ambio*, *51*(2), 333–344. https://doi.org/10.1007/s13280-021-01667-y

Tatler, B., O'Carroll, D. C., & Laughlin, S. B. (2000). Temperature and the temporal resolving power of fly photoreceptors. *Journal of Comparative Physiology A*, *186*(4), 399–407. https://doi.org/10.1007/s003590050439

Tesi, T., Muschitiello, F., Mollenhauer, G., Miserocchi, S., Langone, L., Ceccarelli, C., Panieri, G., Chiggiato, J., Nogarotto, A., Hefter, J., Ingrosso, G., Giglio, F., Giordano, P., & Capotondi, L. (2021). Rapid Atlantification along the Fram Strait at the beginning of the 20th century. *Science Advances*, *7*(48), eabj2946. https://doi.org/10.1126/sciadv.abj2946

Varpe, Ø., Daase, M., & Kristiansen, T. (2015). *Fish-eye view on the new Arctic lightscape | ICES Journal of Marine Science | Oxford Academic*. ICES Journal of Marine Science. https://academic.oup.com/icesjms/article/72/9/2532/2457864

Viljanen, M. L., Nevala, N. E., Calais-Granö, C. L., Lindström, K. M., & Donner, K. (2017). Increasing the illumination slowly over several weeks protects against light damage in the eyes of the crustacean Mysis relicta. *Journal of Experimental Biology | The Company of Biologists*. https://journals.biologists.com/jeb/article/220/15/2798/17902/Increasing-the-illumination-slowly-over-several

Volent, Z., Johnsen, G., & Sigernes, F. (2007). *Kelp forest mapping by use of airborne hyperspectral imager*.

Wallace, M. I., Cottier, F. R., Berge, J., Tarling, G. A., Griffiths, C., & Brierley, A. S. (2010). Comparison of zooplankton vertical migration in an ice-free and a seasonally ice-covered Arctic fjord: An insight into the influence of sea ice cover on zooplankton behavior. *Limnology and Oceanography*, *55*(2), 831–845. https://doi.org/10.4319/lo.2010.55.2.0831

Warrant, E. J., & Johnsen, S. (2013). Vision and the light environment. *Current Biology*, *23*(22), R990–R994. https://doi.org/10.1016/j.cub.2013.10.019

Widder, E. A., Latz, M. I., & Case, J. F. (1983). Marine Bioluminescence Spectra Measured with an Optical Multichannel Detection System. *Bio Bull,* 165(3), 791-810. https://doi.org/10.2307/1541479

Zar, J. H. (2010). *Biostatical Analysis* (5th ed.). Pearson Education Inc.

Appendix A

LINEAR REGRESSION RESULTS

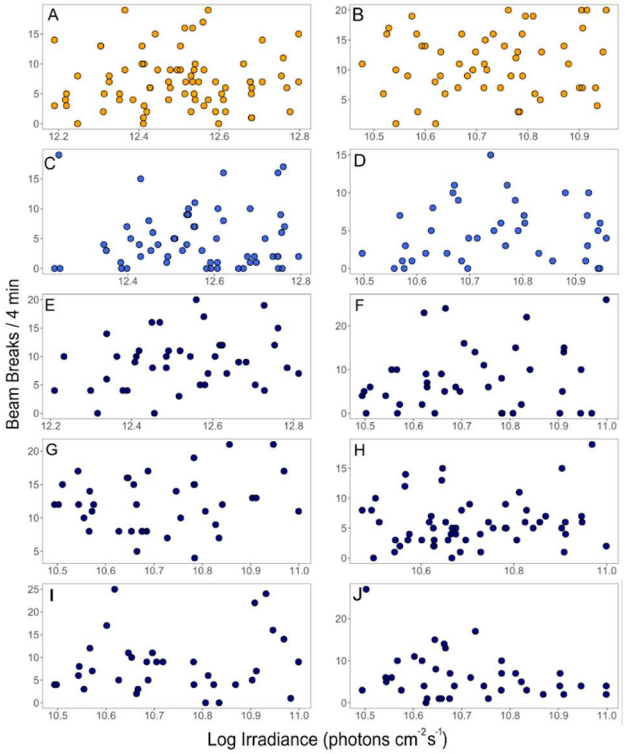

Figure A1: Activity per LAM Position Irradiance Value for All Experimental Trials. Every individual in an experiment is tested at a specific irradiance value per their position in the LAM light field. Irradiance measurements were conducted using a Gamma Scientific UDT 247 Sensor at each LAM position. Colors correspond to sampled stations (MS-S: orange, PN-S: blue, PN-F: dark blue). Beam breaks per 4 minutes at each experimental group's peak activity point are plotted as a function of each individual's assigned irradiance value in an experimental set up. Experiments include **(A)** MS-S spectral experiment, **(B)** MS-S irradiance experiment, **(C)** PN-S spectral, **(D)** PN-S irradiance, **(E)** PN-F spectral, **(F)** PN-F irradiance, **(G)** PN-F 6°C irradiance, **(H)** PN-F -1°C irradiance, **(I)** PN-F day irradiance, and **(J)** PN-F nighttime irradiance.

Table A1: Linear Regression Results for Activity vs. LAM Position Irradiance Value. A linear regression was conducted to test activity as a function of irradiance across the LAM light field per experimental trial. The regression was conducted on each individual's beam breaks per the 4-minute period at their experimental group's peak activity against their tested irradiance value in an experiment. P values ($p < 0.05$) per experiment and season/station are listed in the table below. No significant correlation between irradiance exposure and activity was found in any of the experimental trials.

Season/Station	Experiment (Panel Reference)	p-value
Midnight Sun		
MS-S	Spectral Response **(A)**	0.8077
	Irradiance Response **(B)**	0.3508
Polar Night		
PN-S	Spectral Response **(C)**	0.8508
	Irradiance Response **(D)**	0.7117
PN-F	Spectral Response **(E)**	0.2043
	Irradiance Response **(F)**	0.2837
	6°C Irradiance Response **(G)**	0.1936
	-1°C Irradiance Response **(H)**	0.2656
	Day Irradiance Response **(I)**	0.4285
	Night Irradiance Response **(J)**	0.07558

Appendix B

SPECTRAL RESPONSE BETWEEN LOCATIONS DURING POLAR NIGHT

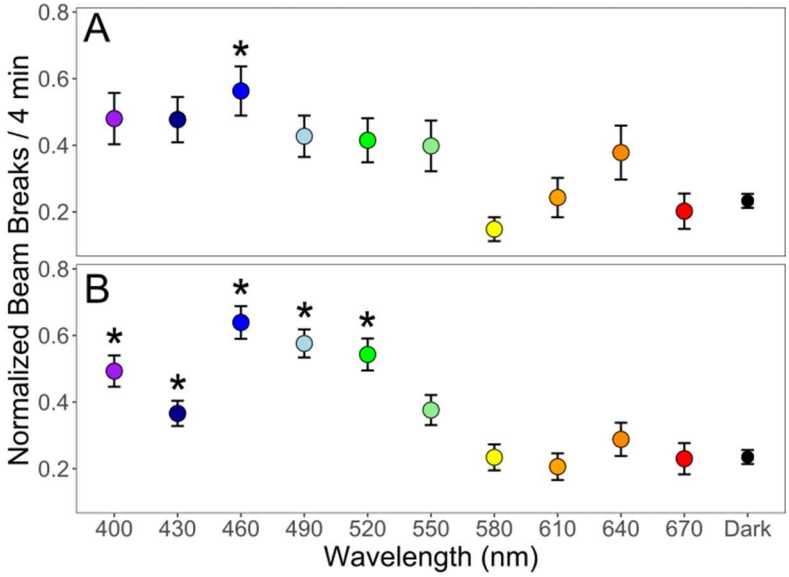

Figure B1: Spectral Response Across Location During Polar Night. Swimming response is plotted against wavelengths (400 - 670 nm) for females tested at the **(A)** PN-S and **(B)** PN-F stations. A further description of plot symbols and measures can be found in Figure 2.3.

Appendix C

SPECTRAL AND IRRADIANCE RESPONSE OF TESTED *M. LONGA* MALES

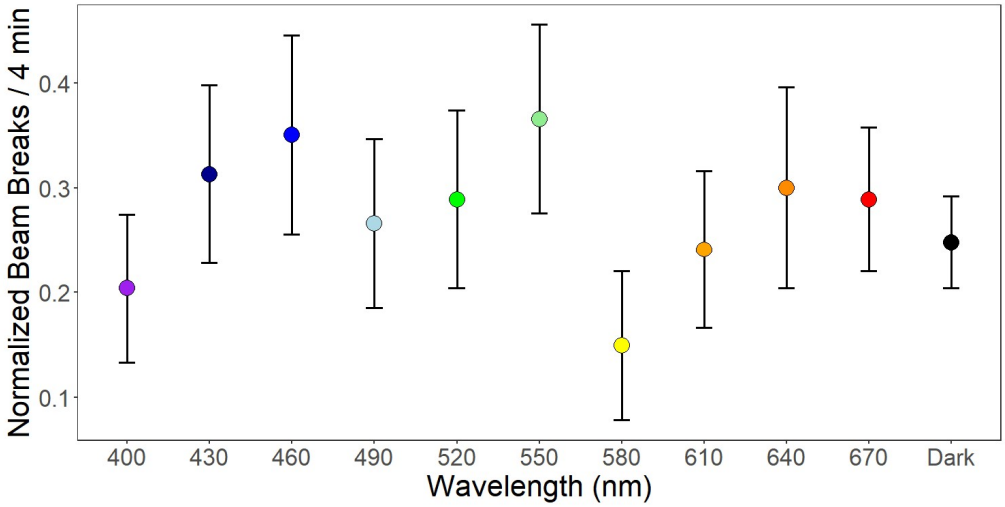

Figure C1: Spectral Response of Male *M. longa* During Polar Night. Swimming response is plotted against wavelength (400 – 670 nm) for males (n = 15) tested at the PN-S station. A further description of plot symbols and measures can be found in Figure 2.3.

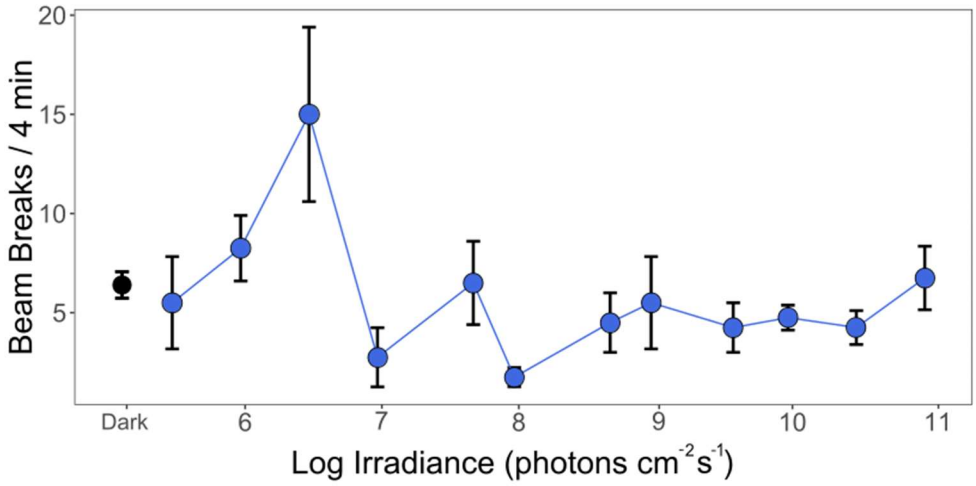

Figure C2: Irradiance Response of Male *M. longa* During Polar Night. Swimming response is plotted against increasing intensities for males (n = 4) tested at the PN-S station. A further description of plot symbols and measures can be found in Figure 2.4. There is an increase in response at 10^6 photons $cm^{-2}s^{-1}$, but a low sample size and high variance at this threshold makes results inconclusive.